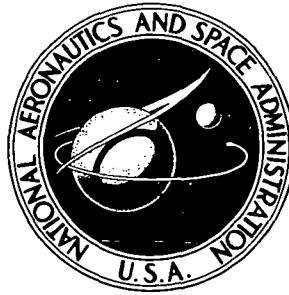


74N11832

**NASA TECHNICAL NOTE**



**NASA TN D-7399**

**NASA TN D-7399**

**WIND-TUNNEL INVESTIGATION OF  
AN UPPER SURFACE BLOWN JET-FLAP  
POWERED-LIFT CONFIGURATION**

*by*

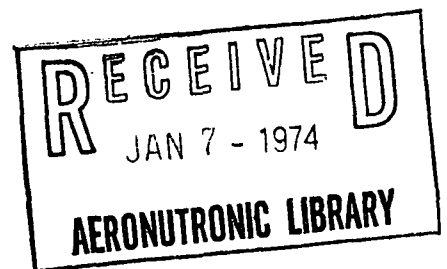
*Arthur E. Phelps III*

*Langley Directorate, U.S. Army Air Mobility R&D Laboratory  
Hampton, Va. 23665*

*and*

*Charles C. Smith, Jr.*

*Langley Research Center  
Hampton, Va. 23665*



1. Report No. NASA TN D-7399		2. Government Accession No.		3. Recipient's Catalog No.	
4. Title and Subtitle WIND-TUNNEL INVESTIGATION OF AN UPPER SURFACE BLOWN JET-FLAP POWERED-LIFT CONFIGURATION				5. Report Date December 1973	
				6. Performing Organization Code	
7. Author(s) Arthur E. Phelps III (Langley Directorate, U.S. Army Air Mobility R&D Laboratory) and Charles C. Smith, Jr. (Langley Research Center)				8. Performing Organization Report No. L-9051	
				10. Work Unit No. 760-61-02-01	
9. Performing Organization Name and Address NASA Langley Research Center Hampton, Va. 23665				11. Contract or Grant No.	
				13. Type of Report and Period Covered Technical Note	
12. Sponsoring Agency Name and Address National Aeronautics and Space Administration Washington, D.C. 20546				14. Sponsoring Agency Code	
				15. Supplementary Notes	
16. Abstract  An investigation has been conducted in the Langley full-scale tunnel to determine the performance and static stability and control characteristics of a four-engine, upper surface blown jet-flap powered-lift configuration with a swept wing. The investigation included test performed over a range of angle of attack ( $-4^{\circ}$ to $36^{\circ}$ ), angle of sideslip ( $-5^{\circ}$ to $5^{\circ}$ ), and thrust coefficients (0 to 4.32) for both symmetric and engine-out power conditions and for horizontal and vertical tails both on and off.  In addition to the four-engine tests, a few tests were made with the outboard engines removed to simulate a twin-engine powered-lift transport configuration.					
17. Key Words (Suggested by Author(s)) STOL Jet flap Propulsive lift Upper surface blowing Over-the-wing blowing			18. Distribution Statement Unclassified - Unlimited		
19. Security Classif. (of this report) Unclassified		20. Security Classif. (of this page) Unclassified		21. No. of Pages 61	22. Price* Domestic, \$3.50 Foreign, \$6.00

# WIND-TUNNEL INVESTIGATION OF AN UPPER SURFACE BLOWN JET-FLAP POWERED-LIFT CONFIGURATION

By Arthur E. Phelps III  
Langley Directorate, U.S. Army Air Mobility R&D Laboratory  
and Charles C. Smith, Jr.  
Langley Research Center

## SUMMARY

An investigation has been conducted in the Langley full-scale tunnel to determine the performance and static stability and control characteristics of an upper surface blown jet-flap powered-lift configuration. The model had an aspect-ratio-7 swept wing and had four simulated high-bypass-ratio turbofan engines mounted in nacelles having rectangular nozzles. The top of the nozzle exit was contoured so that the exhaust flow was deflected downward toward the top of the wing for better spreading and flattening of the exhaust over the wing and flaps. In addition, a few tests were performed with the outboard engines removed to simulate a twin-engine configuration.

The results of the investigation showed that the high lift coefficients necessary for powered-lift operation could be achieved with the test configuration and that the performance was generally comparable to that of other externally blown high-lift concepts in which the engine exhaust flow is fairly well localized inboard on the wing. The use of contoured nacelles, which deflected the jet exhaust downward on top of the wing, in combination with a relatively large flap turning radius was found to be effective for turning the engine exhaust flow over the trailing-edge flaps. A horizontal tail mounted on top of the vertical tail provided longitudinal trim at all lift coefficients and longitudinal stability up to relatively high lift coefficients. Tail-on directional stability and effective dihedral were positive for all power settings at all angles of attack below the stall.

## INTRODUCTION

In the late 1950's, considerable research was conducted at the Langley Research Center to provide basic information on jet-augmented flaps; included in that work were tests on a configuration in which all the jet efflux was exhausted externally over the top of the wing and deflected downward by trailing-edge flaps. The results of that work, which

included both aerodynamic and noise tests, showed that the concept provided good aerodynamic efficiency and, because the wing tended to shield the engine noise from the ground, offered advantages for minimizing the noise associated with powered lift. (See refs. 1 and 2.)

Although the early research effort on jet-augmented flaps provided encouraging results with respect to performance, there was little interest in powered-lift aircraft at that time because of the comparatively poor thrust-weight ratios of early turbojet engines and because there were considerable high-temperature structural problems associated with their use. The fairly recent development of efficient turbofan engines with relatively cool exhausts has greatly minimized these problems, and there has developed a renewed interest in the application of the jet-augmented flap as a means of improving the take-off and landing performance of jet-transport aircraft. Of particular interest at the present time is the upper surface blown jet-flap (USB) concept because it appears to offer promise in reducing the noise of powered-lift aircraft. However, the use of such engines results in a relatively thick, low-pressure-ratio jet which differs considerably from the thin, high-pressure jets of earlier investigations, and there is some question as to the effectiveness of the concept when high-bypass-ratio engines are used. The results of a recent investigation which was conducted to provide some preliminary information on the effectiveness of the concept with high-bypass-ratio engines are reported in reference 3. The investigation of reference 3 utilized the semispan test technique and showed that the use of engine-exhaust deflectors mounted on top of the nacelle to flatten and spread the jet exhaust was effective for maintaining flow attachment over the flaps and for producing the high lift necessary for powered-lift operation. The present investigation is an extension to the preliminary work reported in reference 3. Emphasis is placed on providing performance information obtained with a full-span model and on providing some fundamental data on the stability, control, and engine-out trim problems of the USB concept.

The present investigation was performed over a range of angle of attack, angle of sideslip, and thrust coefficients for both symmetric and engine-out power conditions and for the horizontal and vertical tails on and off. The model was equipped with four simulated high-bypass-ratio engines mounted in nacelles having moderate-aspect-ratio (width-height ratio) rectangular nozzles. The top of the nacelle at the nozzle exit was contoured so that the exhaust flow was deflected downward toward the top of the wing for better spreading and flattening of the exhaust over the wing and flaps. The model had a full-span leading-edge slat and trailing-edge double-slotted flap. The slots in the trailing-edge flaps directly behind the engines were covered by using thin sheet metal over the flaps. Some engine-out tests were performed with this sheet metal removed behind the failed engine in order to investigate the effects of opening the flap slots behind the dead engine.

In addition to the four-engine tests, a few tests were made with the outboard engines removed to simulate a twin-engine powered-lift configuration.

### SYMBOLS

The longitudinal data are referred to the stability-axis system and the lateral data are referred to the body-axis system. (See fig. 1.) The origin of the axes was located to correspond to the center-of-gravity position (0.40 mean aerodynamic chord) shown in figure 2. Measurements were made in U.S. Customary Units. They are presented herein in the International System of Units (SI) with the equivalent values in U.S. Customary Units given parenthetically:

$b$	wing span, m (ft)
$c$	local wing chord, m (ft)
$\bar{c}$	mean aerodynamic chord, m (ft)
$C_D$	drag coefficient, $F_D/qS$
$C_L$	lift coefficient, $F_L/qS$
$C_{L,trim}$	lift coefficient with pitch trim supplied by a lift load on a tail $3.5\bar{c}$ rearward of the center of gravity
$C_l$	rolling-moment coefficient, $M_X/qSb$
$C_m$	pitching-moment coefficient, $M_Y/qS\bar{c}$
$C_n$	yawing-moment coefficient, $M_Z/qSb$
$C_Y$	side-force coefficient, $F_Y/qS$
$C_\mu$	gross static thrust coefficient, $T/qS$
$C_{l_\beta} = \frac{\partial C_l}{\partial \beta}$	per degree
$C_{n_\beta} = \frac{\partial C_n}{\partial \beta}$	per degree

$$C_{Y\beta} = \frac{\partial C_Y}{\partial \beta}, \text{ per degree}$$

$F_A$	net axial force, N (lb)
$F_D$	drag force, N (lb)
$F_L$	lift force, N (lb)
$F_N$	normal force, N (lb)
$F_R$	resultant force, $\sqrt{F_N^2 + F_A^2}$ , N (lb)
$F_Y$	side force, N (lb)
$i_t$	horizontal-tail incidence angle, deg
$M_X$	rolling moment, m-N (ft-lb)
$M_Y$	pitching moment, m-N (ft-lb)
$M_Z$	yawing moment, m-N (ft-lb)
$q$	free-stream dynamic pressure, $N/m^2$ (lb/ft <sup>2</sup> )
$S$	wing area, m <sup>2</sup> (ft <sup>2</sup> )
$T$	installed static thrust, N (lb)
$W$	weight, N (lb)
$X, Y, Z$	body reference axes
$X_S, Y_S, Z_S$	stability reference axes
$\alpha$	angle of attack, deg
$\beta$	angle of sideslip, deg
$\gamma$	flight-path angle, $-\tan^{-1}(C_D/C_L)$ , deg

$\delta_e$	elevator deflection (positive if trailing edge down), deg
$\delta_f$	total deflection of double-slotted flap, deg
$\delta_j$	jet-deflection angle, deg
$\eta$	flap-system turning efficiency, $F_R/T$

Abbreviations:

USB	upper surface blown jet flap
EBF	externally blown jet flap
WRP	wing reference plane

### MODEL AND APPARATUS

The present investigation was conducted on the four-engine, high-wing model shown in figure 2(a). This model was originally intended for use in a test program of an externally blown jet-flap (EBF) configuration (see ref. 4), but it was modified to the USB configuration shown in figure 2(a) by moving the engines to the upper surface of the wing at the same spanwise stations intended for the EBF arrangement. The horizontal and vertical tails denoted by dotted lines in figure 2(a) were tested to investigate only potential stability and control problems and were not optimized for this investigation.

Figure 2(b) presents details of the engine-nacelle arrangement used in the tests. The top of the exhaust nozzle was contoured so that the exhaust-flow center line was deflected downward toward the top of the wing; and the sides of the nacelle were flared outward in order to maintain the proper exit area for the turbofan simulators being used. Most of the tests were performed with the basic nacelle, which had an exhaust-nozzle aspect ratio of 4.5; however, some additional tests were performed with the external deflector shown in figure 2(c).

The model had an aspect-ratio-7 wing with  $30^\circ$  leading-edge sweep and incorporated a leading-edge slat (fig. 2(c)) and a full-span double-slotted trailing-edge flap (fig. 2(d)). In order to close the flap slots behind the engines and provide a smooth contour for the exhaust jet to follow, a thin piece of sheet metal was used to fair over the double-slotted trailing-edge flaps in the area immediately behind the engine as shown in figures 2(a) and 2(c). The model was equipped with two different leading-edge slats: the basic slat, which

had a chord of 19 percent of the local wing chord; and a large-chord slat, which had a chord of 25 percent of the local wing chord. The positions of the slat and trailing-edge flaps were set in accordance with the results of previous tests on EBF models and were not necessarily the best positions for the USB model. The trailing-edge flaps were constructed with the fixed gaps, overlaps, and deflection angles shown in figure 2(d). Dimensional characteristics of the model are presented in table I and coordinates for the vane and flap, whose airfoil sections were identical, are presented in table II. The wing used an NACA 4415 airfoil section.

Photographs of the model installed in the test section of the 9.1- by 18.3-meter (30- by 60-ft) open-throat test section of the Langley full-scale tunnel are shown in figure 3.

## TESTS AND PROCEDURES

In preparation for the tests, engine calibrations were made to determine the installed static thrust of each engine as a function of engine rotational speed. These calibrations were made with the engines installed in the nacelles on top of the wing, with trailing-edge flaps removed, and with bellmouth inlets installed on the engines. The installed static thrust was computed to be the resultant of the normal and axial forces ( $\text{Thrust} = \sqrt{F_N^2 + F_A^2}$ ). Tests were then run by setting the engine rotational speed to give the desired thrust and holding these speeds constant over the angle-of-attack range.

Tests were first made at zero airspeed to determine flap turning angles and turning efficiencies under static conditions. These static tests and the wind-on tests were made with the trailing-edge flaps set at deflection angles of  $35^\circ$  and  $55^\circ$ . Wind-on tests were made over an angle-of-attack range from  $-4^\circ$  to  $36^\circ$  for a thrust-coefficient range from 0 to 4.32; sideslip tests were made over a sideslip-angle range from  $-5^\circ$  to  $5^\circ$ . Engine-out tests were run over a range of angle of attack and thrust coefficients in order to investigate the effects of asymmetric thrust on the lateral trim characteristics of the model. Some of these tests were run with the sheet-metal fairing of figures 2(a) and 2(c) removed in the area directly behind the failed engine. Longitudinal and lateral tests were made with the horizontal and vertical tails on and off. In addition to the four-engine arrangement, a few tests were also made with the outboard engines removed to simulate a two-engine powered-lift configuration. Also included in the investigation were tests to determine the effects of slat chord and of an external exhaust deflector on the aerodynamic characteristics of the model. The free-stream dynamic pressure for the tests was  $158 \text{ N/m}^2$  ( $3.31 \text{ lb/ft}^2$ ) for an airspeed of 16 m/sec ( $52.5 \text{ ft/sec}$ ) and a Reynolds number of  $2.98 \times 10^5$ , based on the mean aerodynamic chord.

No wind-tunnel jet-boundary corrections were considered necessary since the model was very small relative to the test-section size.

## RESULTS AND DISCUSSION

### Static Turning

The results of tests to determine the static turning efficiency and turning angle are presented in figure 4 as plots of the ratio of normal force to thrust  $F_N/T$  against the ratio of net axial force to thrust  $-F_A/T$ . The data of figure 4(a) show that a jet turning angle of about  $35^\circ$  to  $40^\circ$  and an efficiency  $\eta$  of 94 percent were obtained for a nominal flap deflection of  $35^\circ$ . For this flap setting, the deflection of the upper surface of the flap relative to the model center line is about  $55^\circ$ . The data indicate that the resultant-force vector, and, therefore, the net jet reaction, is not turned through the full deflection of the flap upper surface even though tufts attached to the flap surface directly behind the engine indicated that the surface flow was attached to the flap. Smoke-flow and tuft studies on this model indicated that the jet grew progressively thicker as it turned over the flap, and this appears to be responsible for the deviation of the resultant vector from the surface of the flap. Although the precise mechanics of this thickening are not known at present, it appears to be due to entrainment of ambient air and a progressive vortex rollup at the sides of the jet sheet.

With either inboard or outboard engines inoperative, the jet turning angle was reduced, but the turning efficiency remained high. The data of figure 4(b) show that the turning angle for the  $55^\circ$  flap setting (flap upper surface deflection of  $75^\circ$ ) was about  $48^\circ$  with both inboard and outboard engines running and that the turning efficiency was about 90 percent. With either inboard or outboard engines inoperative, the turning angle was reduced but the turning efficiency remained high, as was the case for the take-off flap condition. The addition of a deflector to the top of the nacelle in an attempt to increase the spreading for the inboard-engine condition increased the turning angle slightly for this condition but reduced the efficiency to about 80 percent. It should be pointed out that these efficiencies are based on the static thrust of the engine and nacelle installed on the wing, and they do not account for any installation losses.

### Lift Characteristics

The basic longitudinal aerodynamic characteristics of the model with the horizontal tail off are presented in figures 5, 6, and 7 for flap deflections of  $55^\circ$ ,  $35^\circ$ , and  $0^\circ$ , respectively. These data show that an increase in the thrust coefficient caused the usual increase in maximum lift coefficient, stall angle of attack, and negative pitching-moment coefficient.

The model with 55° flap deflection produced lift coefficients up to 9.0 (untrimmed) at a gross thrust coefficient of 4.32.

The 55° flap condition was tested with the basic nacelle (fig. 5(a)), with an external deflector on top of the nacelle (fig. 5(b)), and with the external deflector and a large-chord leading-edge slat (fig. 5(c)). A comparison of the data of these figures (see fig. 8) shows that either the external deflector or the large-chord slat had a relatively small effect on the aerodynamic performance of the four-engine configuration for lift coefficients below about 5.5. Near the stall, however, both the deflector and the slat resulted in improved aerodynamic performance. In addition to the four-engine arrangement, the 55° flap condition was tested with the two outboard engines removed to simulate a two-engine arrangement (figs. 5(d) and 5(e)). The aerodynamic performance with these different engine arrangements is summarized in figure 9. These data show that changes in the engine arrangement had little effect on the aerodynamic performance at low lift coefficients; but, at the stall, the two-engine configurations experienced a loss in maximum lift coefficient for the basic leading-edge slat condition. The combination of deflectors and a large-chord leading-edge slat appears to have provided an improvement in maximum lift coefficient more for the two-engine arrangement than for the four-engine arrangement; however, the four-engine configuration still provided the highest lift.

A comparison of the lift-drag polars of the present model with those of the semispan USB model of reference 3 and with those of a full-span EBF model is presented in figure 10. These data show that the performance of the model of reference 3 is generally in good agreement with that of the model of the present investigation. Also, the data show that the performance of the USB concept is generally comparable to that of the EBF concept.

The aerodynamic performance of the model is summarized in figure 11 in terms of lift-drag polars. The data of figure 11(a) show that for a landing-approach lift coefficient of 4.0, the 55° flap configuration could descend along a 6.0° glide path at a value of  $C_{\mu}$  of about 1.0 and retain an angle-of-attack margin of about 12°. If the maximum installed thrust-weight ratio is assumed to be 0.60, then the maximum climb angle at this flap setting and lift coefficient with full power is about 8°. With an engine out, the climb angle at a thrust-weight ratio of 0.45 is reduced to a small positive value. The data of figure 11(b) show that by changing the flap deflection to 35°, a maximum climb angle of 12° is possible at a lift coefficient of 4 with an installed thrust-weight ratio of 0.6. The climb angle is decreased to about 5° for an engine-out thrust-weight ratio of 0.45 if no performance loss occurs in laterally trimming the aircraft.

#### Longitudinal Stability and Trim

The results of longitudinal stability and trim tests are presented in figures 12 and 13. These tests were made with the tail arrangement shown by the dashed lines in the

three-view drawing presented in figure 2(a). This tail configuration was not optimized for the model but was tested only to investigate potential longitudinal stability and trim problems that may be associated with the upper surface blown-flap concept. The significant points to be made about the data of figures 12 and 13 are that the model can be trimmed in pitch at all lift coefficients and that longitudinal stability can be achieved up to relatively high lift coefficients with the particular tail arrangement chosen for the tests. These results are generally similar to those of the externally blown jet-flap concept using a comparable horizontal tail for trim. (For example, see ref. 5.)

### Lateral Stability

Plots of the static lateral stability derivatives against angle of attack are presented in figures 14 and 15 for the tail-off and tail-on configurations, respectively. The tail-off data of figure 14 show that the application of thrust decreased the directional stability and generally increased the effective dihedral. The tail-on data of figure 15 show positive directional stability at all angles of attack below the stall. As expected, the dihedral effect generally became more positive (larger negative values of  $C_{l\beta}$ ) with the addition of the vertical tail.

### Lateral Moments With One Engine Inoperative

Basic lateral characteristics obtained for the model with one engine inoperative are presented in figures 16 to 19 for the four-engine arrangement with the trailing-edge flaps set at  $55^\circ$ . Similar data with the trailing-edge flaps set at  $35^\circ$  are presented in figures 20 to 23. These basic-data plots also show the effects on the lateral characteristics of opening or closing the trailing-edge flap slots behind the inoperative engine. Since loss of an engine results in loss of lift in a powered-lift system, plots of the lateral characteristics with one engine out are accompanied by plots of the corresponding longitudinal characteristics.

The lateral characteristics with an outboard engine inoperative are summarized in figure 24 and show that, as expected, large rolling moments accompany an engine-out condition. One interesting point noted in this plot is that the rolling moments were larger when the slots behind the inoperative engine were opened. Opening the slots behind the inoperative engine apparently adversely affected the spreading and turning of the flow from the operating engine directly adjacent to the slots. A similar result was obtained with an inboard engine inoperative. (Compare figs. 17 and 19.)

The basic engine-out lateral characteristics for the two-engine arrangement with the flap slots closed and opened behind the inoperative engine are presented in figures 25 and 26, respectively. Figure 27 summarizes the engine-out data for the two-engine

condition and shows that unlike the four-engine condition, opening the slots behind the inoperative engine reduced the engine-out rolling moments slightly. This result was expected since the flow behind the inoperative engine for the two-engine configuration was found to be separated over the flaps with the slots closed.

Figure 28 presents a comparison of the engine-out rolling moments for the four-engine and two-engine configurations at a constant value of thrust-weight ratio of 0.45. Also presented in this figure are engine-out data for an externally blown flap configuration having spanwise engine locations approximately equal to those of the four-engine upper surface blown-flap configuration. This figure emphasizes the large engine-out moments that are inherent in systems using external blowing; and it appears that there is little difference in the magnitude of the engine-out moments whether the engines are located beneath the wing or on top of the wing. One method of reducing these moments is to locate the engines as close inboard on the span as practical, particularly for the two-engine arrangement since in this case the loss of an engine reduces the thrust by one-half and results in large lift losses. It should be pointed out that the results of previous work with an EBF configuration (ref. 5) have shown that a variety of methods are available for trimming the engine-out moments while providing satisfactory maneuvering control power. No lateral trim methods were tested in this investigation but it is possible that some of the lateral trim methods found effective for the EBF concept may be effective for achieving lateral trim and the USB concept.

## SUMMARY OF RESULTS

From a wind-tunnel investigation of an upper surface blown jet-flap powered-lift configuration utilizing high-bypass-ratio turbofan engines, the following results were obtained:

1. The high lift coefficients necessary for powered-lift operation could be achieved with the test configuration, and the performance was generally comparable to that of other externally blown high-lift concepts in which the exhaust flow was fairly well localized inboard on the wing.

2. The use of contoured nacelles, which deflected the jet exhaust downward on top of the wing, in combination with a relatively large flap turning radius was found to be effective for turning the engine-exhaust flow over the trailing-edge flaps.

3. A horizontal tail mounted on top of the vertical tail provided longitudinal trim at all lift coefficients and longitudinal stability up to relatively high lift coefficients.

4. The tail-on effective dihedral was positive for all power settings and generally increased with increasing angle of attack.

5. The tail-on directional stability was positive for all power settings at all angles of attack below the stall.

6. The engine-out rolling moments were large and almost equivalent to those of other externally blown high-lift concepts.

Langley Research Center,  
National Aeronautics and Space Administration,  
Hampton, Va., October 15, 1973.

#### REFERENCES

1. Turner, Thomas R.; Davenport, Edwin E.; and Riebe, John M.: Low-Speed Investigation of Blowing From Nacelles Mounted Inboard and on the Upper Surface of an Aspect-Ratio-7.0  $35^\circ$  Swept Wing With Fuselage and Various Tail Arrangements. NASA MEMO 5-1-59L, 1959.
2. Maglieri, Domenic J.; and Hubbard, Harvey H.: Preliminary Measurements of the Noise Characteristics of Some Jet-Augmented-Flap Configurations. NASA MEMO 12-4-58L, 1959.
3. Phelps, Arthur E.; Letko, William; and Henderson, Robert L.: Low-Speed Wind-Tunnel Investigation of a Semispan STOL Jet Transport Wing-Body With an Upper-Surface Blown Jet Flap. NASA TN D-7183, 1973.
4. Smith, Charles C., Jr.: Effect of Engine Position and High-Lift Devices on Aerodynamic Characteristics of an External-Flow Jet-Flap STOL Model. NASA TN D-6222, 1971.
5. Parlett, Lysle P.; Greer, H. Douglas; Henderson, Robert L.; and Carter, C. Robert: Wind-Tunnel Investigation of an External-Flow Jet-Flap Transport Configuration Having Full-Span Triple-Slotted Flaps. NASA TN D-6391, 1971.

TABLE I.- DIMENSIONS OF MODEL

Fuselage:

Length, m (ft) . . . . .	1.82 (5.96)
Diameter, m (ft) . . . . .	0.155 (0.508)
Distance from nose to center of gravity, m (ft) . . . . .	0.762 (2.500)

Wing:

Aspect ratio . . . . .	7
Area, m <sup>2</sup> (ft <sup>2</sup> ) . . . . .	0.452 (4.86)
Span, m (ft) . . . . .	1.77 (5.833)
Root chord, m (ft) . . . . .	0.372 (1.219)
Tip chord, m (ft) . . . . .	0.136 (0.447)
Mean aerodynamic chord, m (ft) . . . . .	0.272 (0.893)
Distance from wing root to mean aerodynamic chord, m (ft) . . . . .	0.376 (1.233)
Vane chord . . . . .	0.15c
Flap chord . . . . .	0.30c
Sweep, leading edge, deg . . . . .	30

Spanwise engine locations:

Inboard . . . . .	0.27b/2
Outboard . . . . .	0.43b/2

Vertical tail:

Area, m <sup>2</sup> (ft <sup>2</sup> ) . . . . .	0.13 (1.40)
Span, cm (in.) . . . . .	42.7 (16.80)
Root chord, cm (in.) . . . . .	43.2 (17.00)
Tip chord, cm (in.) . . . . .	17.8 (7.00)

Horizontal tail:

Area, m <sup>2</sup> (ft <sup>2</sup> ) . . . . .	0.151 (1.63)
Span, cm (in.) . . . . .	85.34 (33.60)
Chord, cm (in.) . . . . .	17.8 (7.00)
Incidence . . . . .	Variable

TABLE II.- VANE AND FLAP COORDINATES HAVING  
NACA 4415 AIRFOIL SECTIONS

Chordwise station, $x$ , percent chord	Ordinate, $z$ , percent chord	
	Upper surface	Lower surface
0	0	0
5	9.8	-3.3
10	13.0	-4.1
15	15.0	-3.8
20	16.0	-3.8
25	17.2	-3.5
30	17.3	-3.3
40	17.0	-2.8
50	15.2	-2.2
60	12.5	-1.7
70	10.0	-1.3
80	7.1	-.9
90	4.0	-.6
100	1.2	-.3

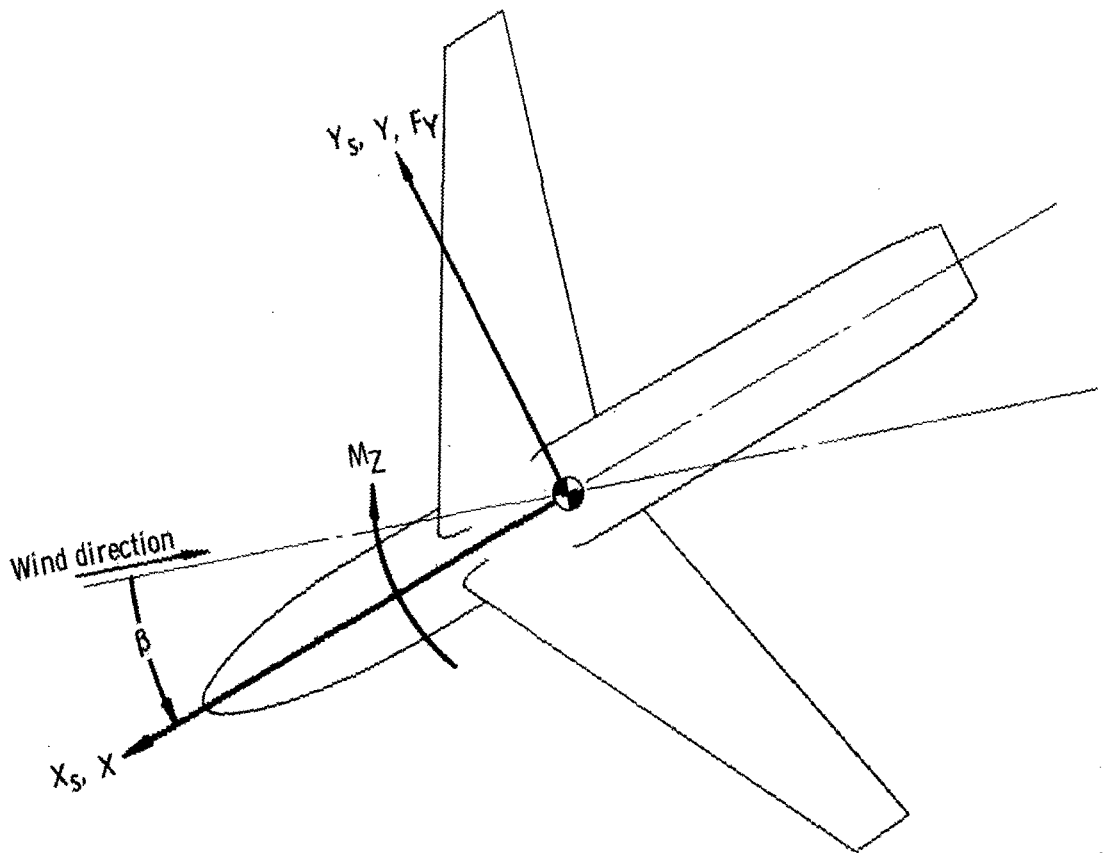
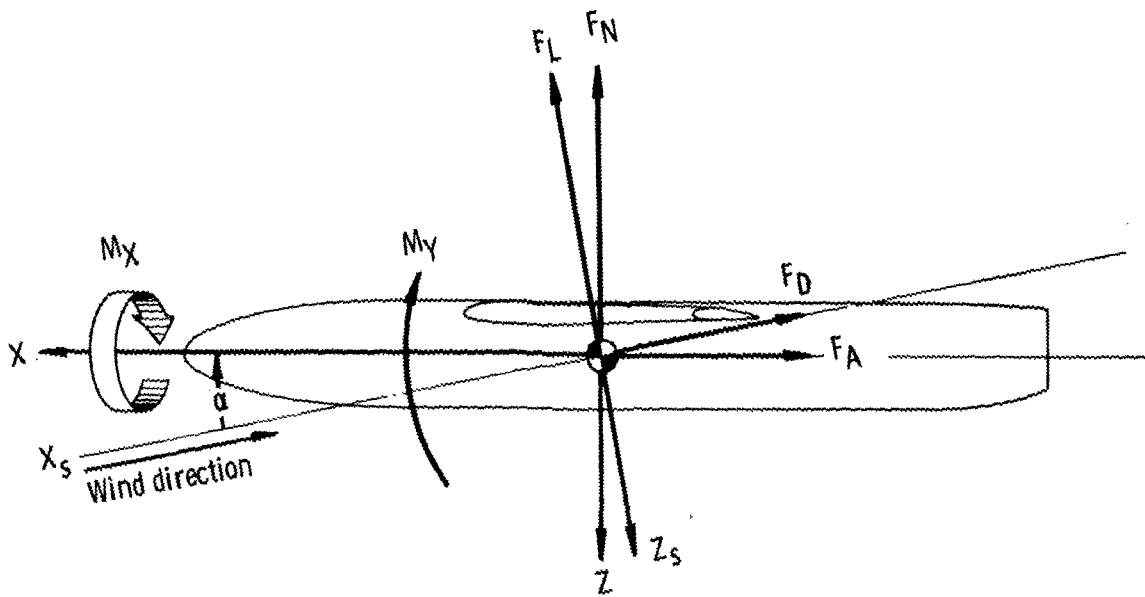
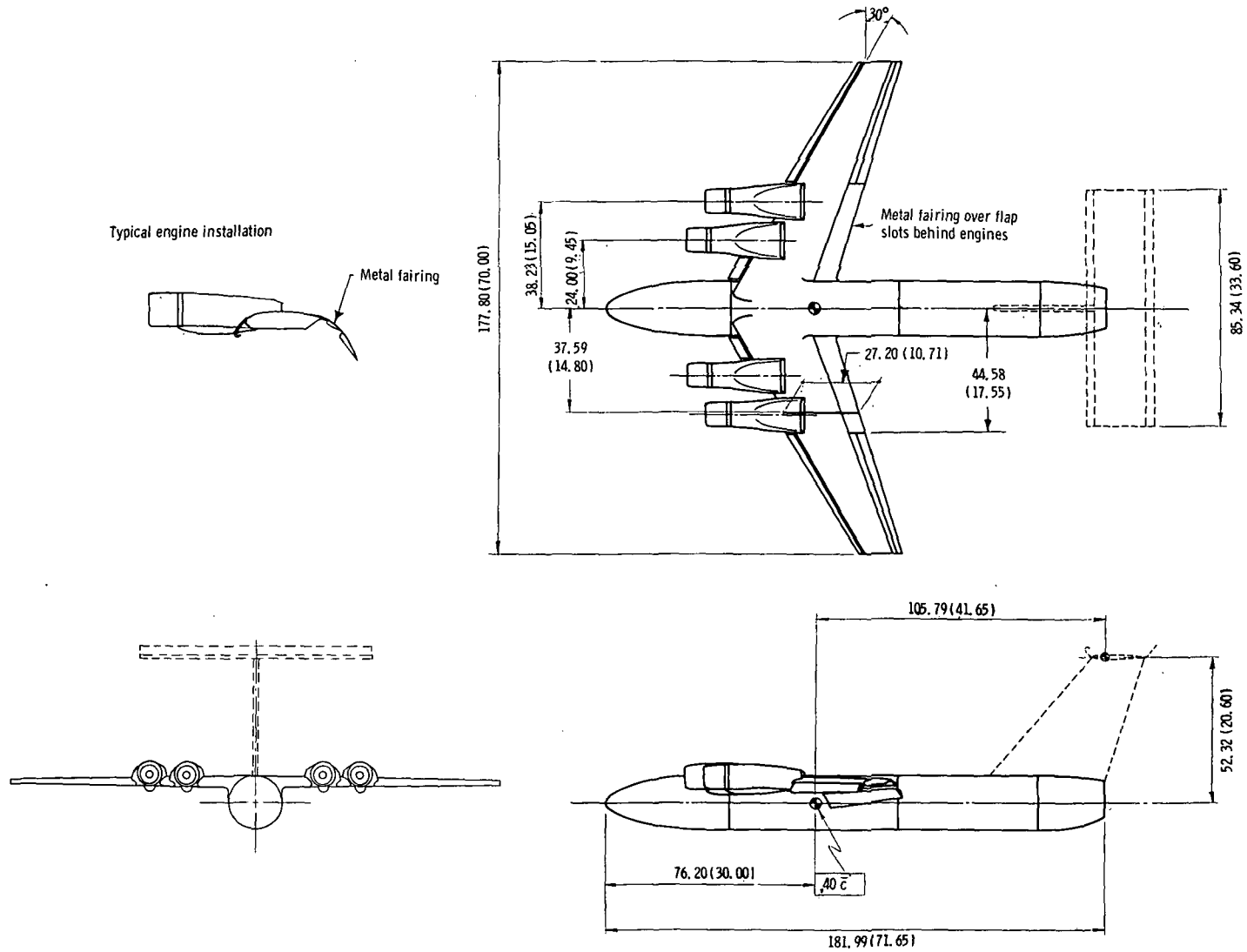
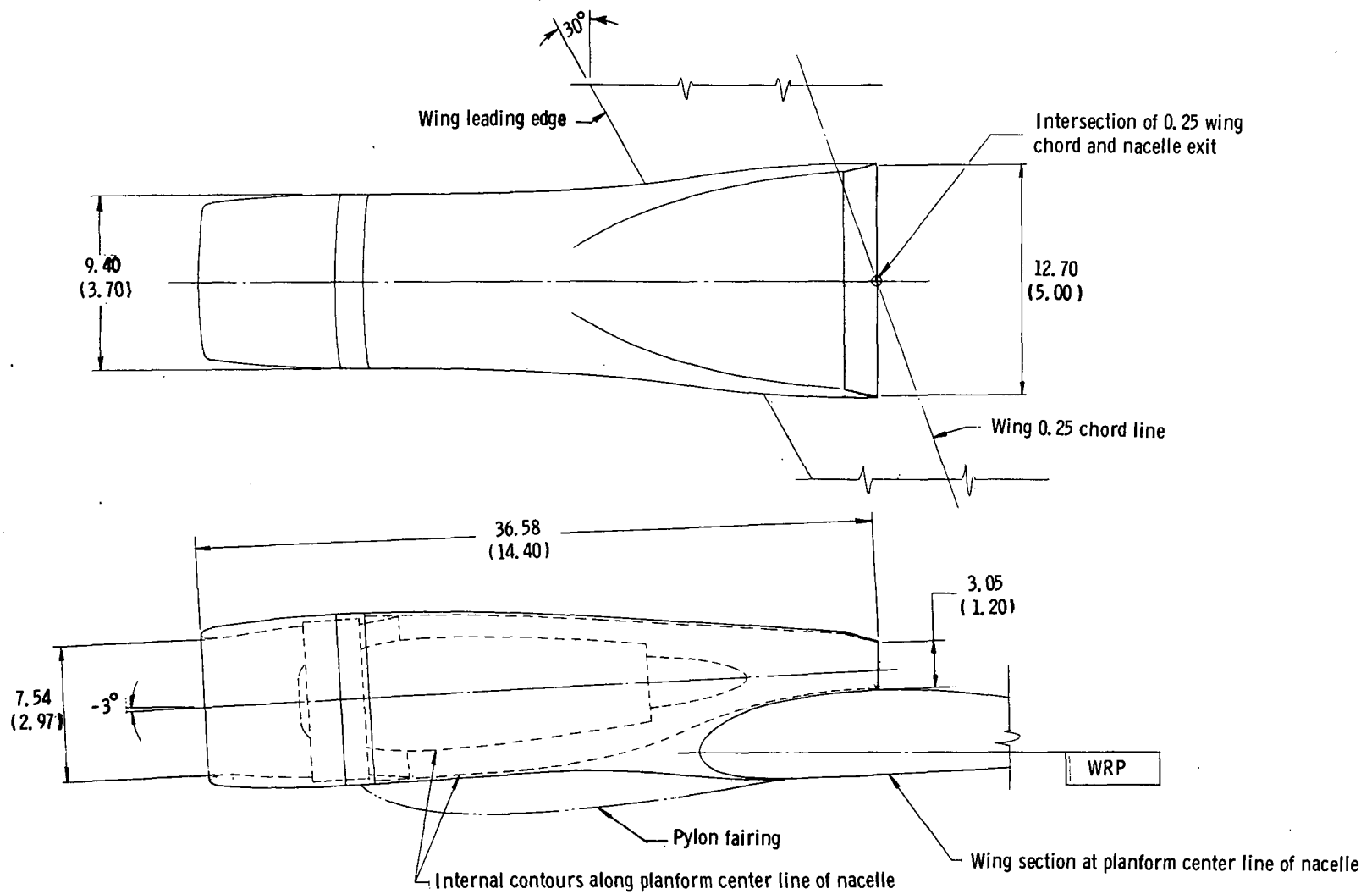


Figure 1.- Axis systems used in presentation of data. Arrows indicate positive direction of forces, moments, axes, and angles.



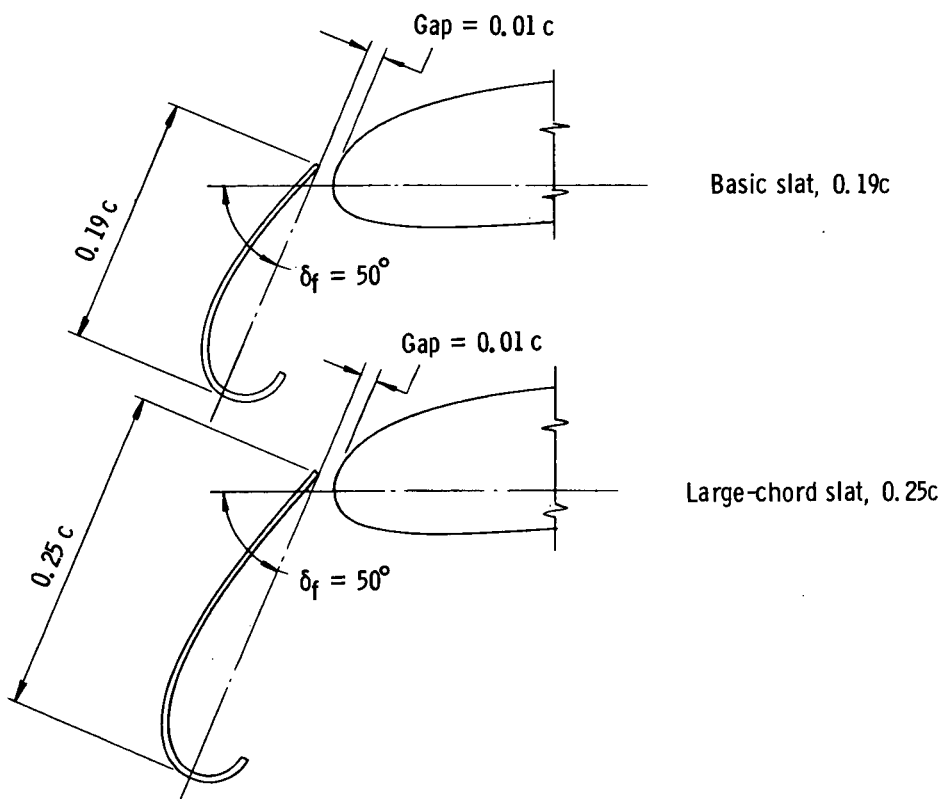
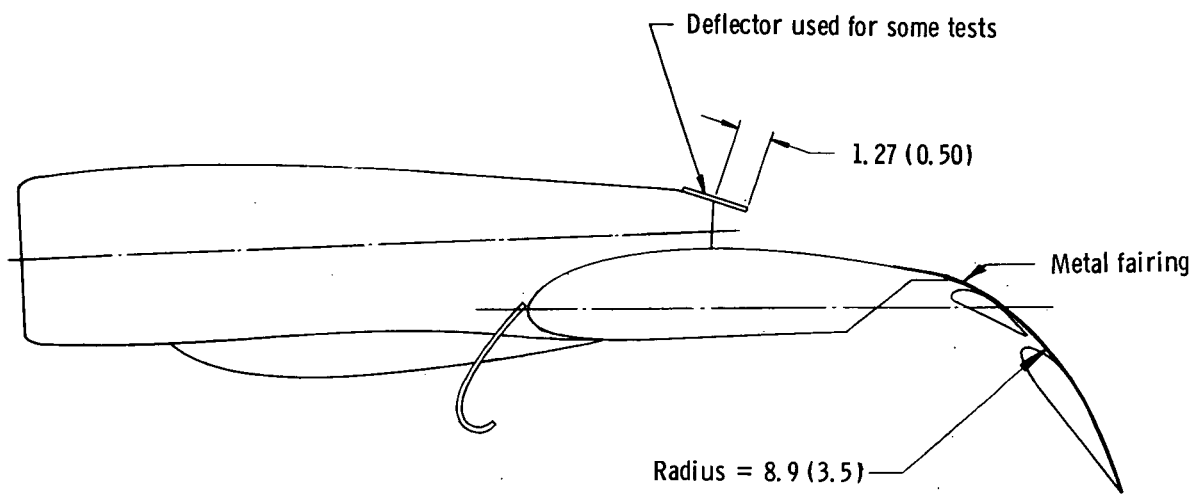
(a) Three-view drawing of model.

Figure 2.- Drawings of model used in investigation. All dimensions are in centimeters (inches).



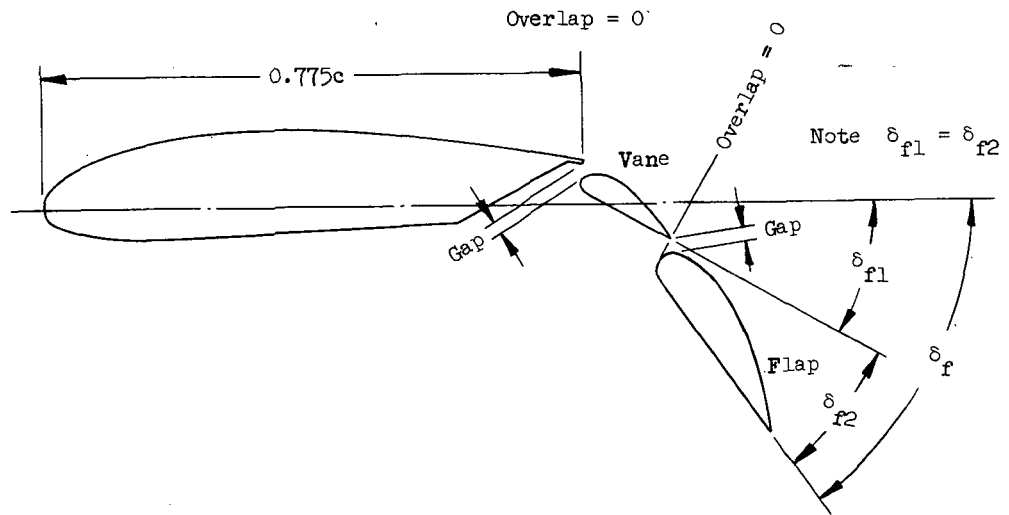
(b) Sketch of basic nacelle showing typical installation on wing.

Figure 2.- Continued.



(c) Details of external deflector and leading-edge slat.

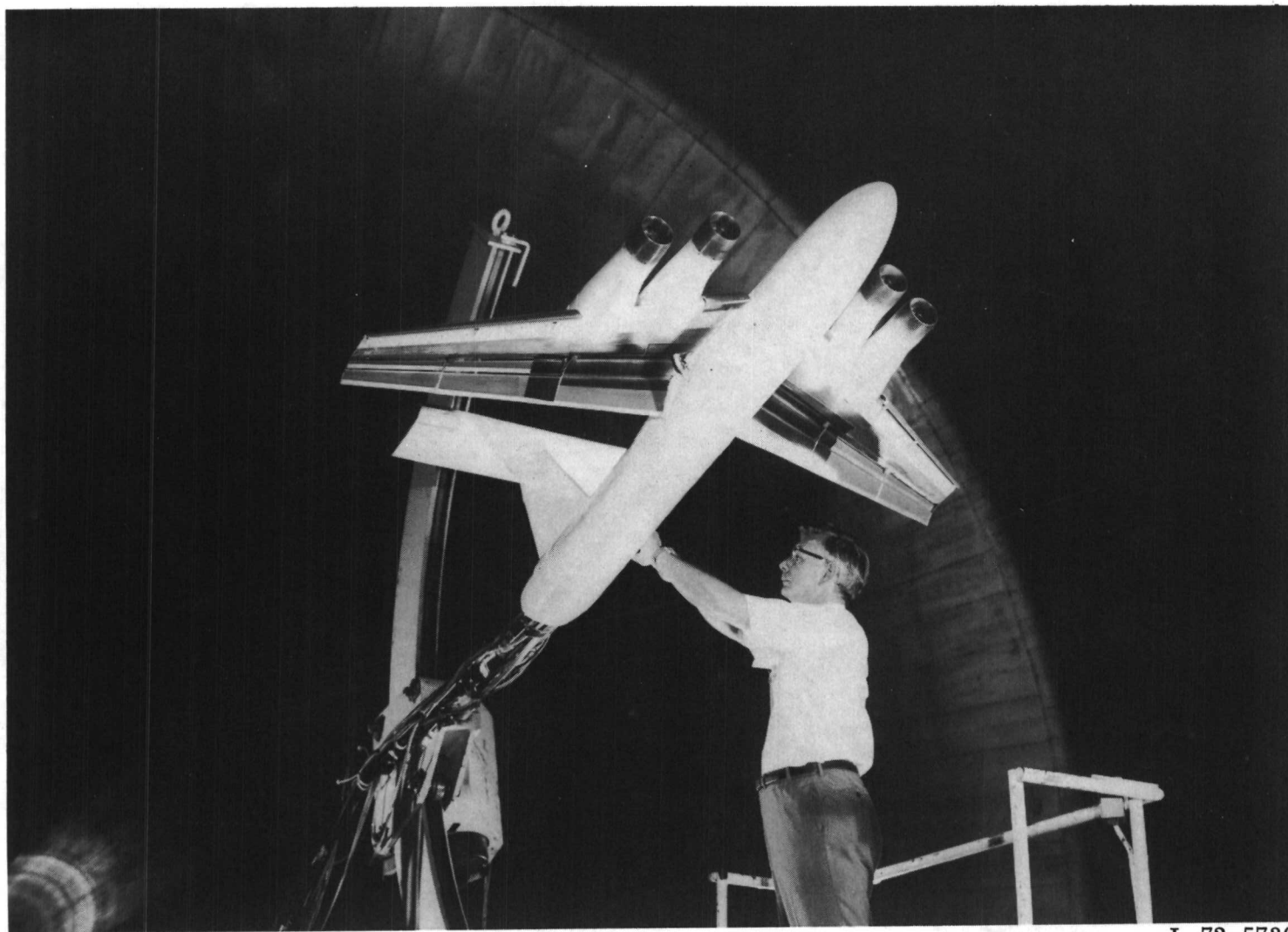
Figure 2.- Continued.



$\delta_{f1}/\delta_{f2}$ , deg	Vane gap, percent $c$	Vane overlap, percent $c$	Flap gap, percent $c$	Flap overlap, percent $c$
17.5/35	2	0	2	0
27.5/55	2	0	2	0

(d) Details of trailing-edge flap.

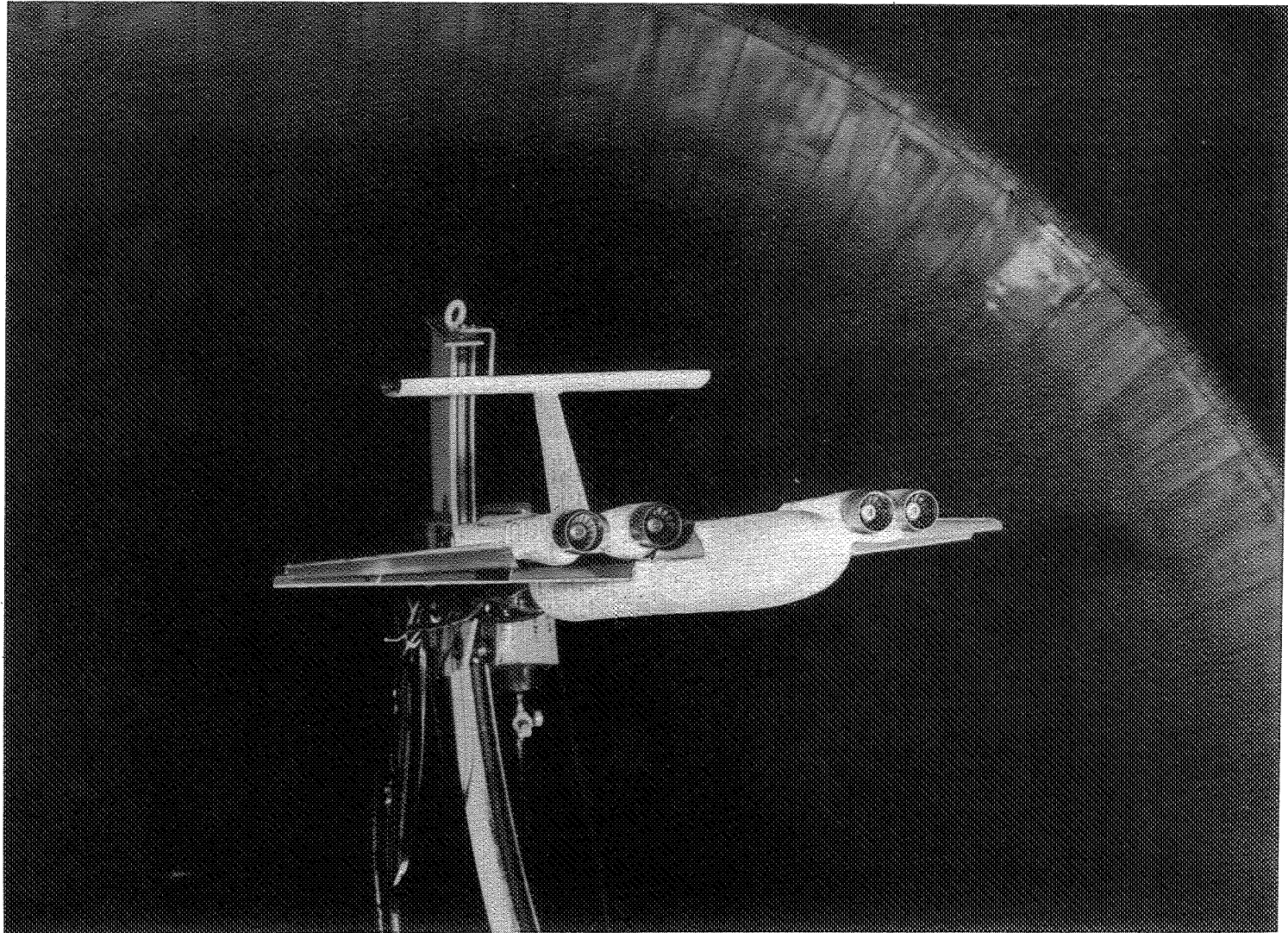
Figure 2.- Concluded.



L-72-5736

(a) Bottom view.

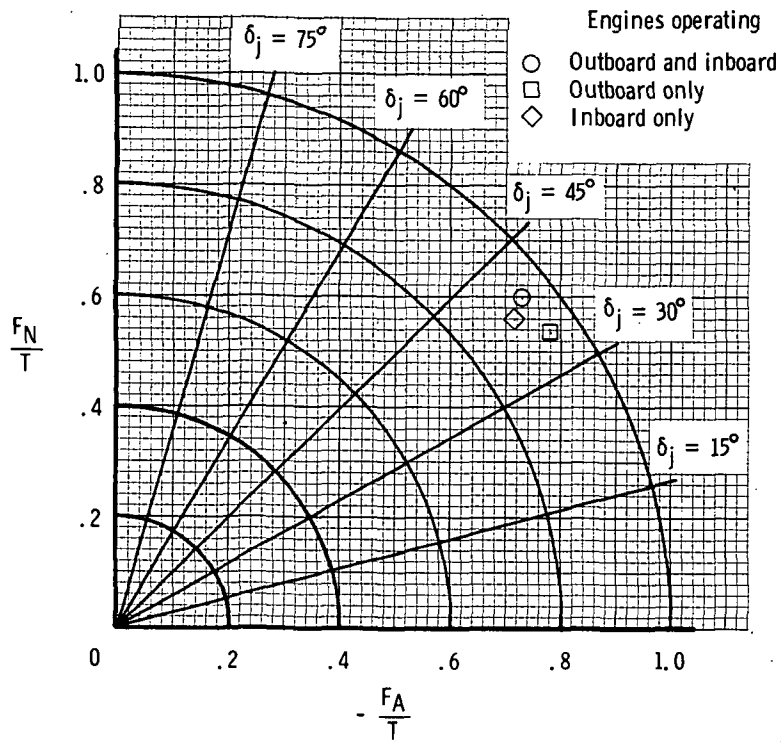
Figure 3.- Photographs of model installed in the Langley full-scale tunnel.



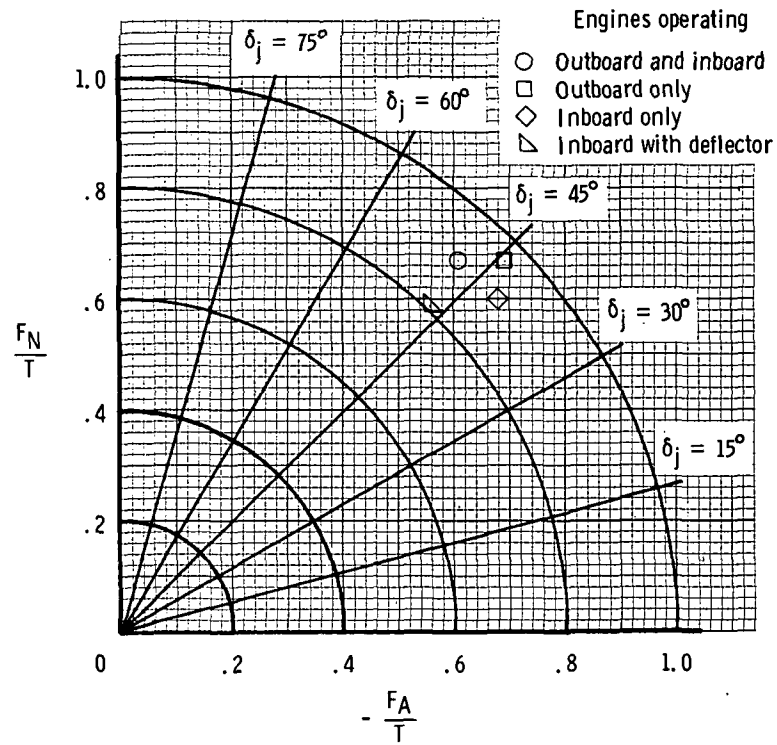
L-72-5738

(b) Three-quarter front view.

Figure 3.- Concluded.

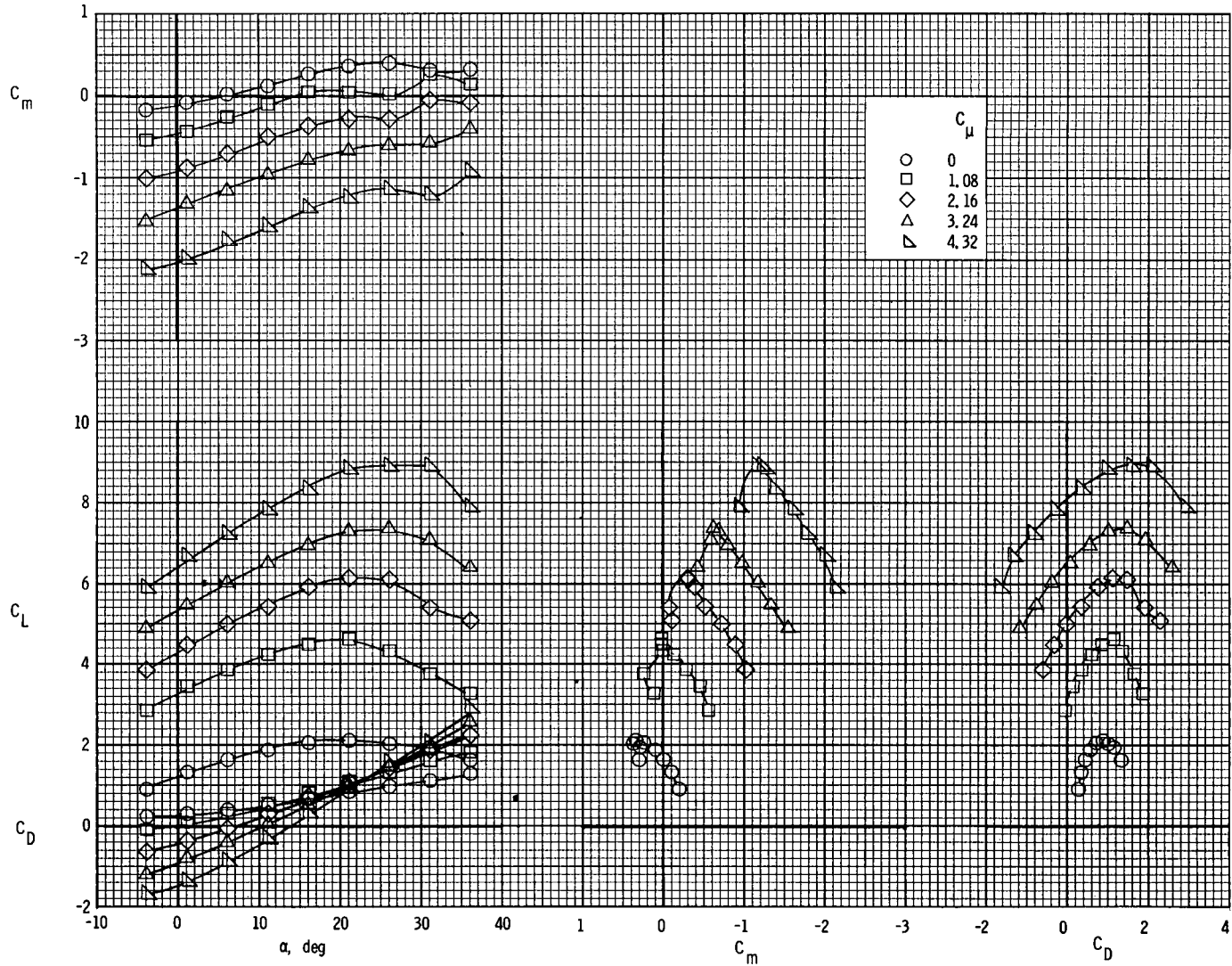


(a)  $\delta_f = 35^\circ$ .



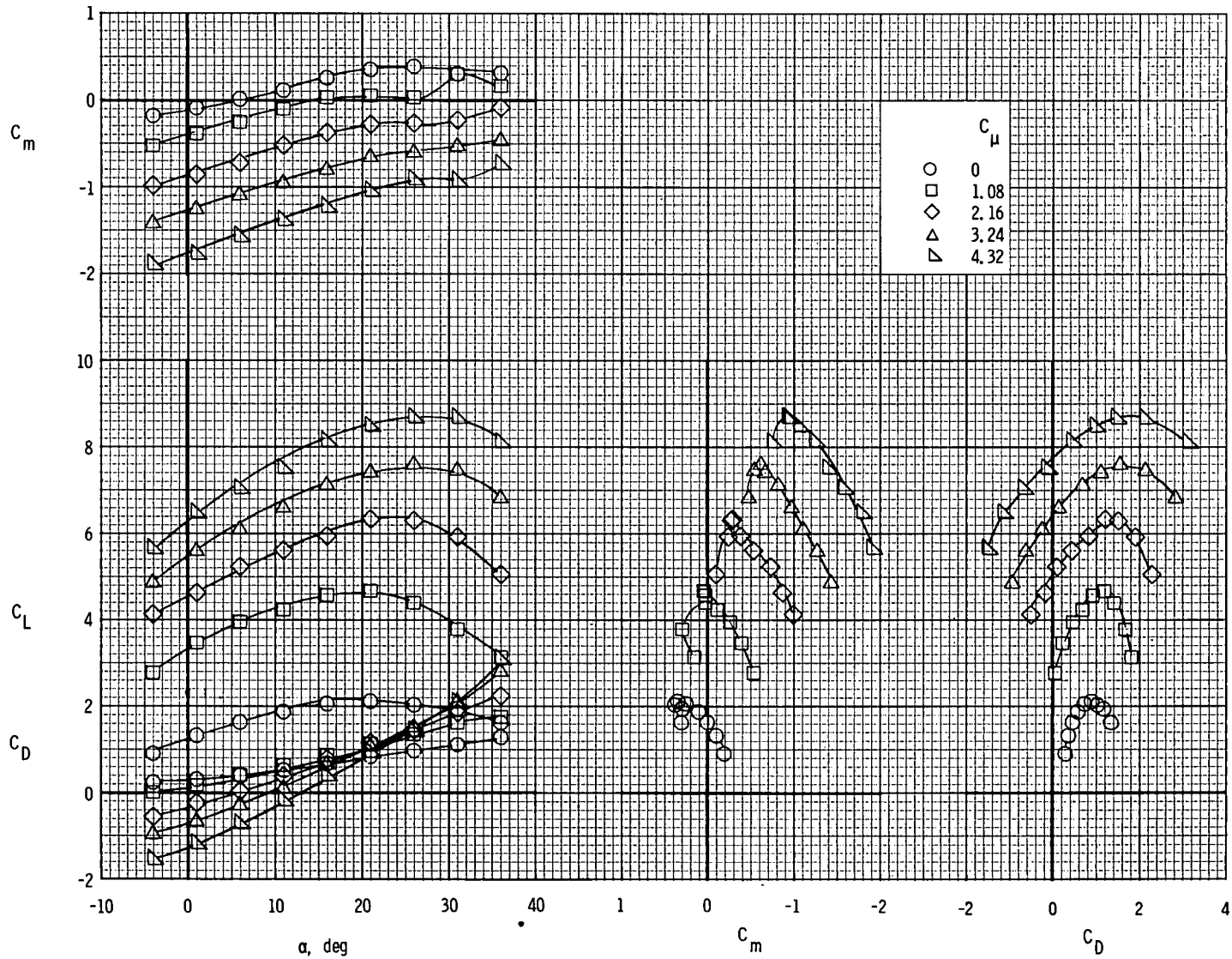
(b)  $\delta_f = 55^\circ$ .

Figure 4.- Summary of flap turning efficiency and turning angle. Full power.



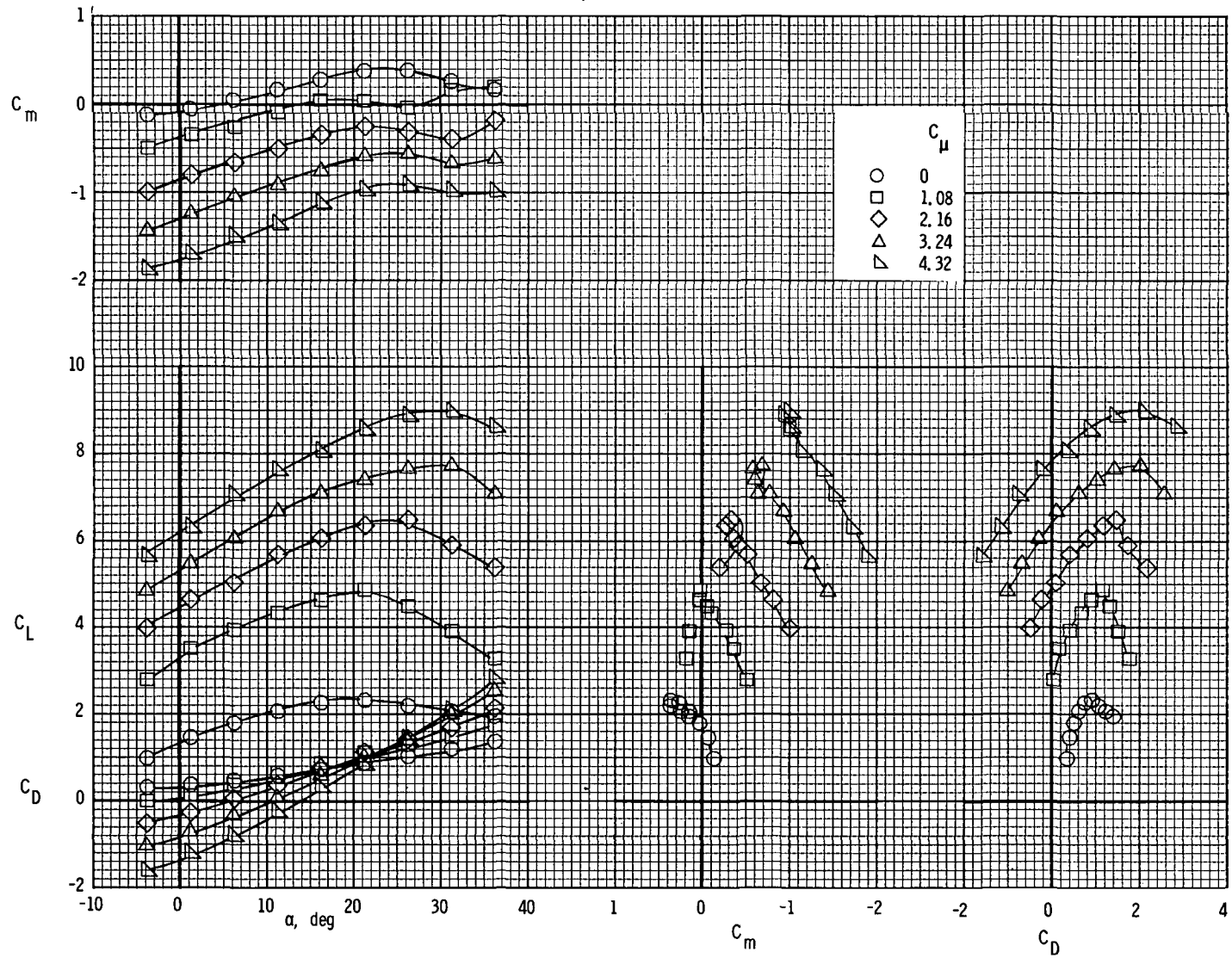
(a) Four-engine arrangement; basic nacelle.

Figure 5.- Longitudinal characteristics of model with horizontal tail off.  $\delta_f = 55^\circ$ .



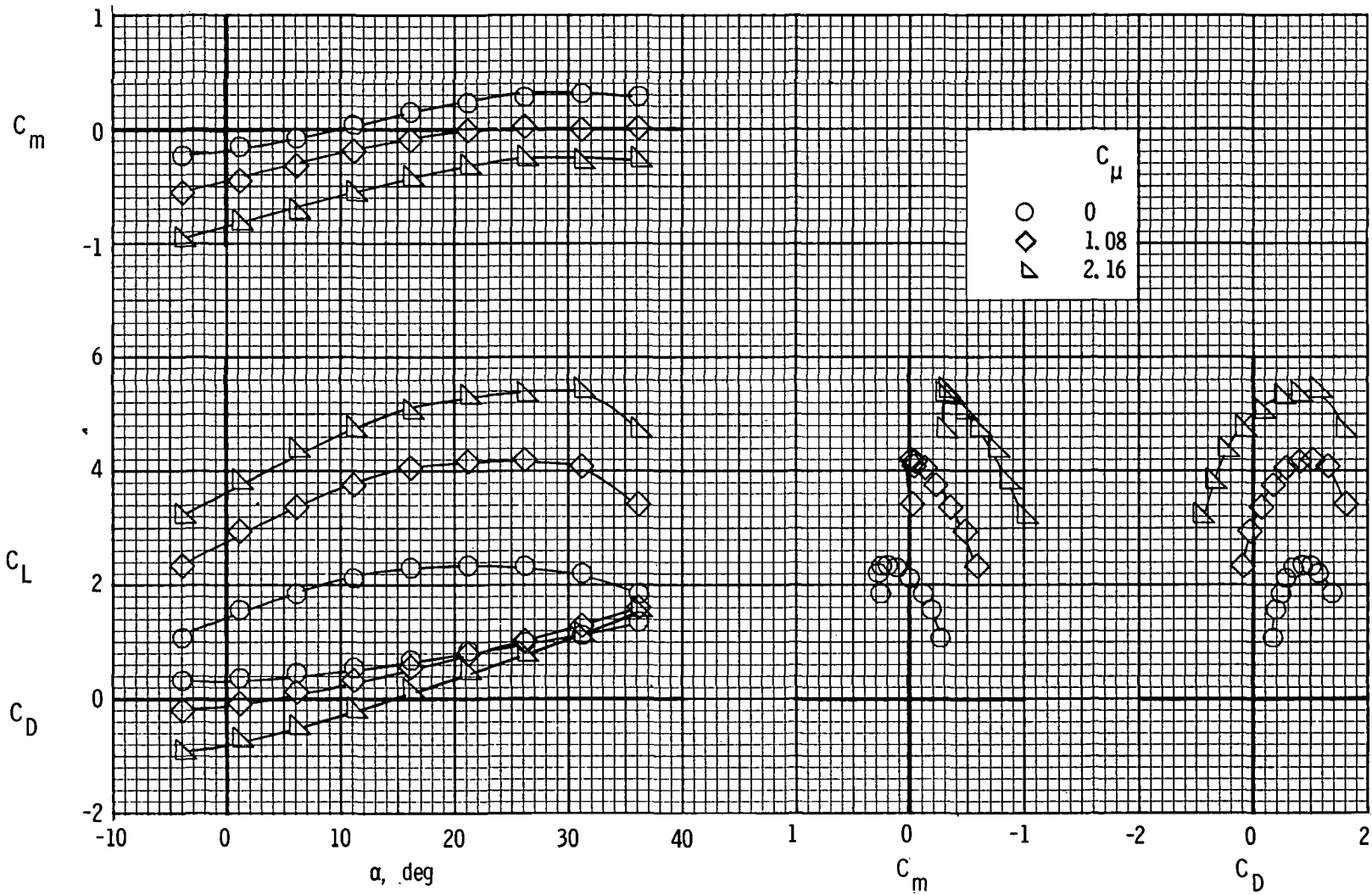
(b) Four-engine arrangement; nacelle deflector.

Figure 5.- Continued.



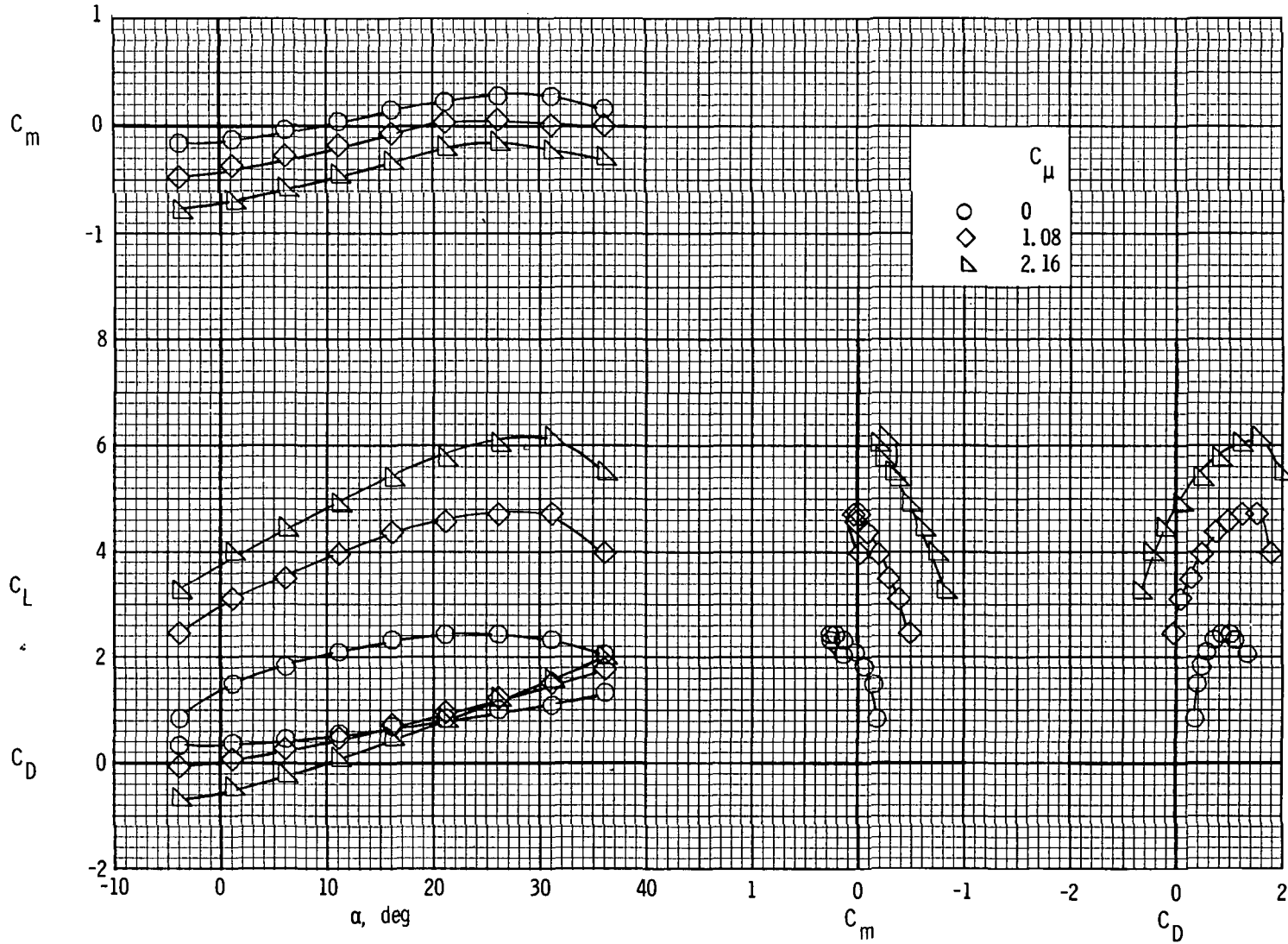
(c) Four-engine arrangement; nacelle deflector; large-chord leading-edge slat.

Figure 5.- Continued.



(d) Two-engine arrangement.

Figure 5.- Continued.



(e) Two-engine arrangement; nacelle deflector; large-chord leading-edge slat.

Figure 5.- Concluded.

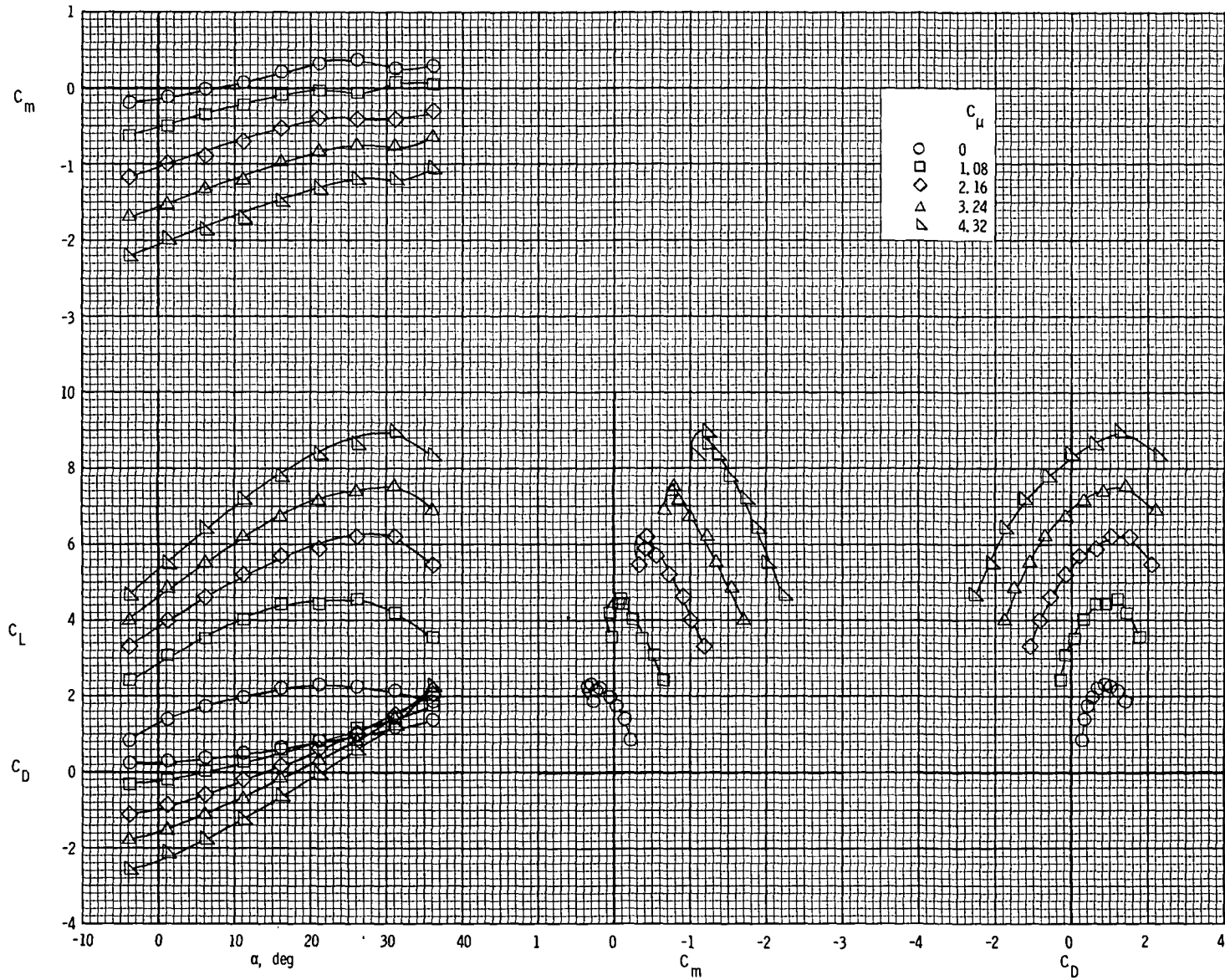


Figure 6.- Longitudinal characteristics of the model with tail off.  $\delta_f = 35^\circ$ .

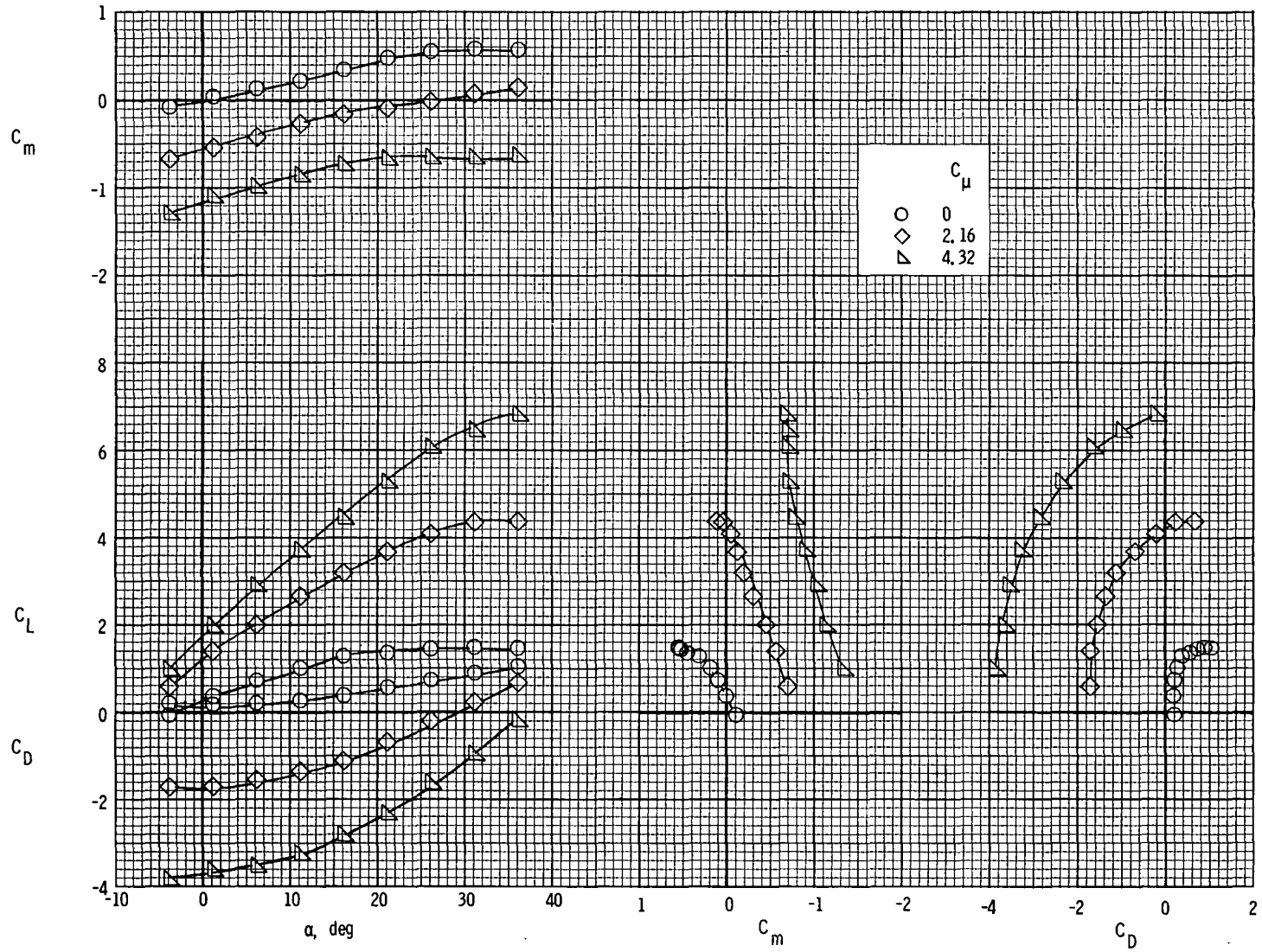


Figure 7.- Longitudinal characteristics of the model with tail off.  $\delta_f = 0^\circ$ .

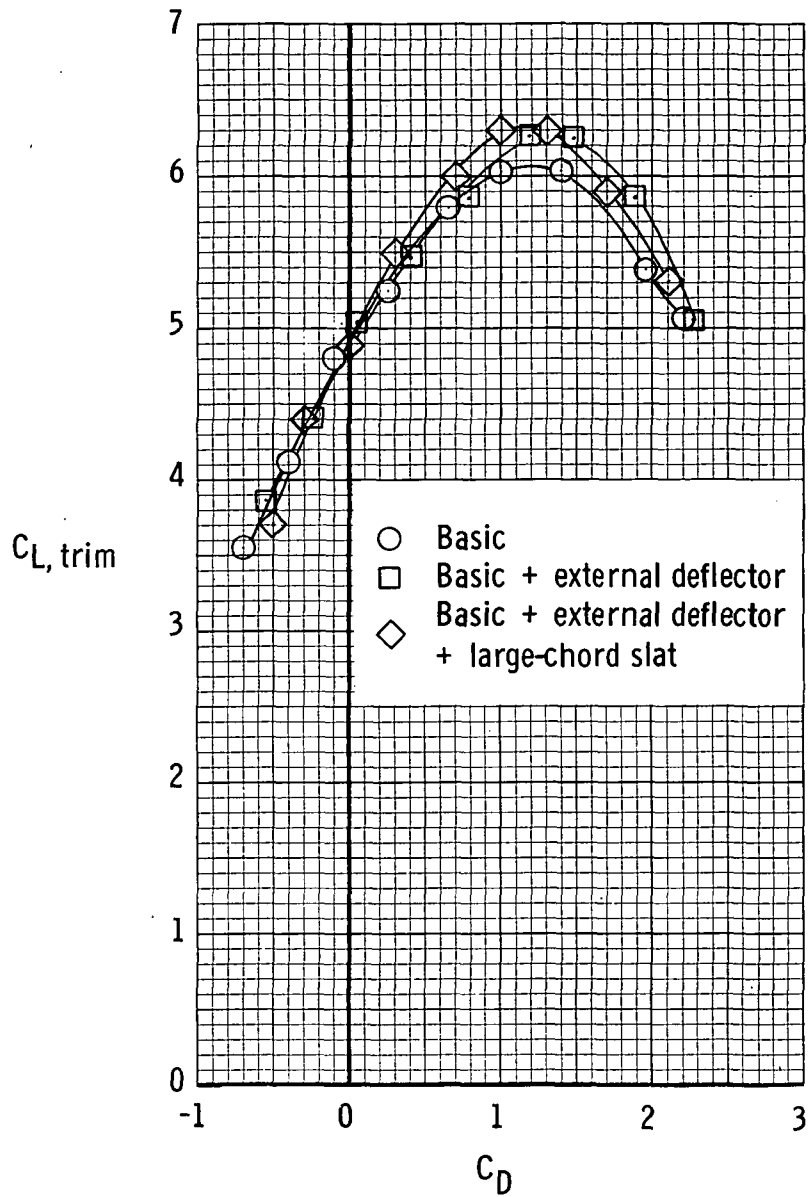
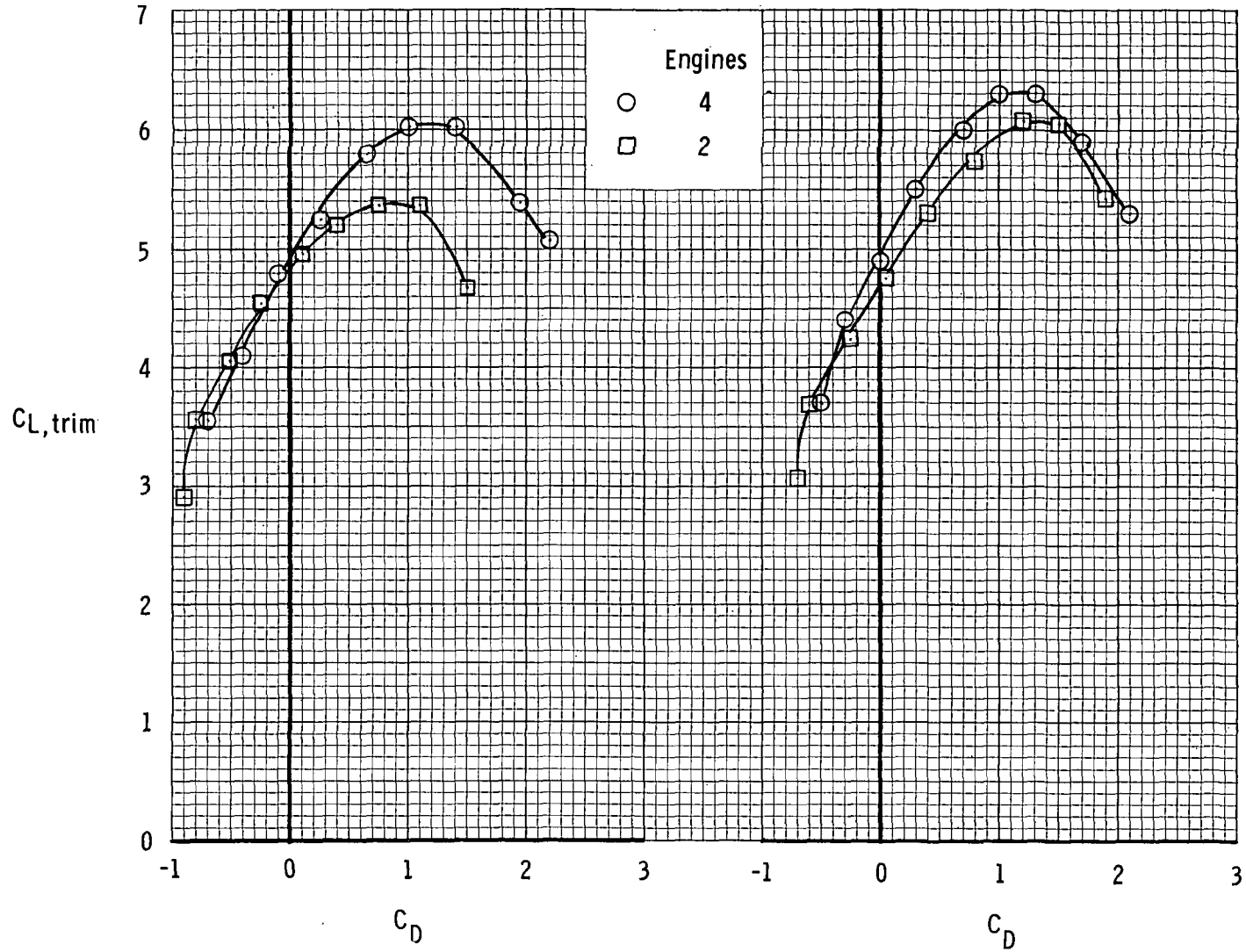


Figure 8.- Effect of external deflector and large-chord slat on performance of basic four-engine configuration.  $\delta_f = 55^\circ$ ;  $C_\mu = 2.16$ .



(a) Basic leading-edge slat.

(b) Extended chord slat and external deflector.

Figure 9.- Comparison of aerodynamic characteristics of four-engine and two-engine configurations.

$$\delta_f = 55^\circ; C_{\mu} = 2.16.$$

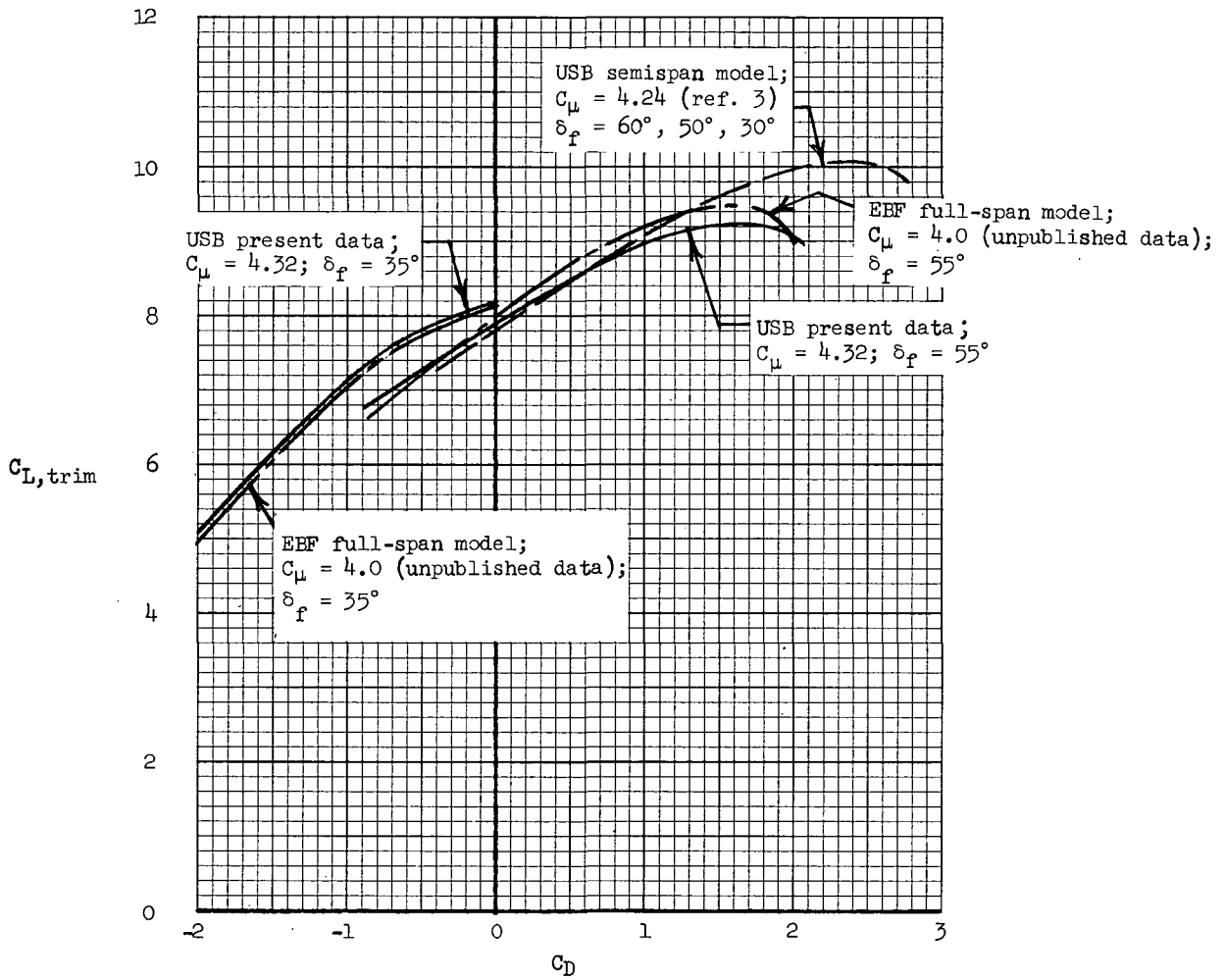
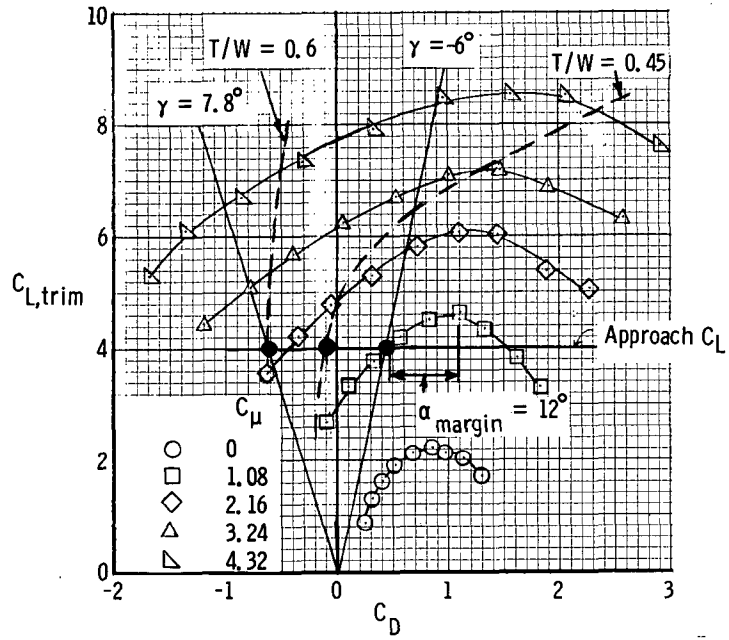
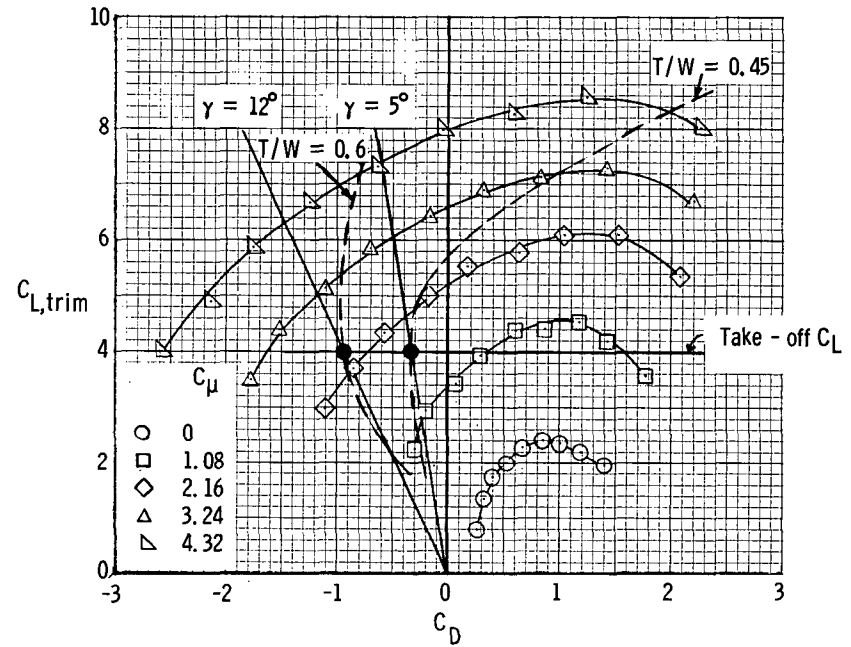


Figure 10.- Comparison of lift-drag characteristics.

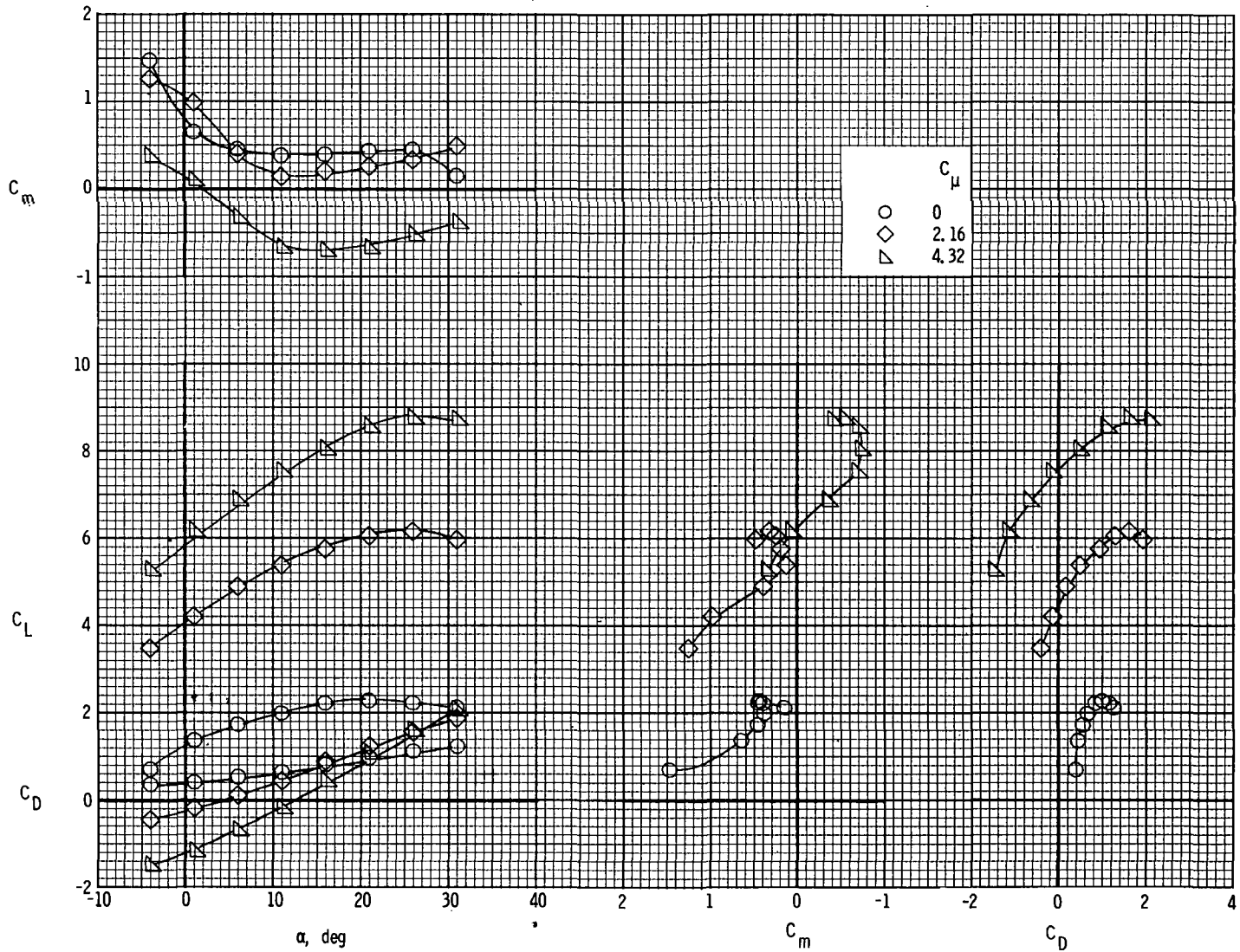


(a)  $\delta_f = 55^\circ$ .



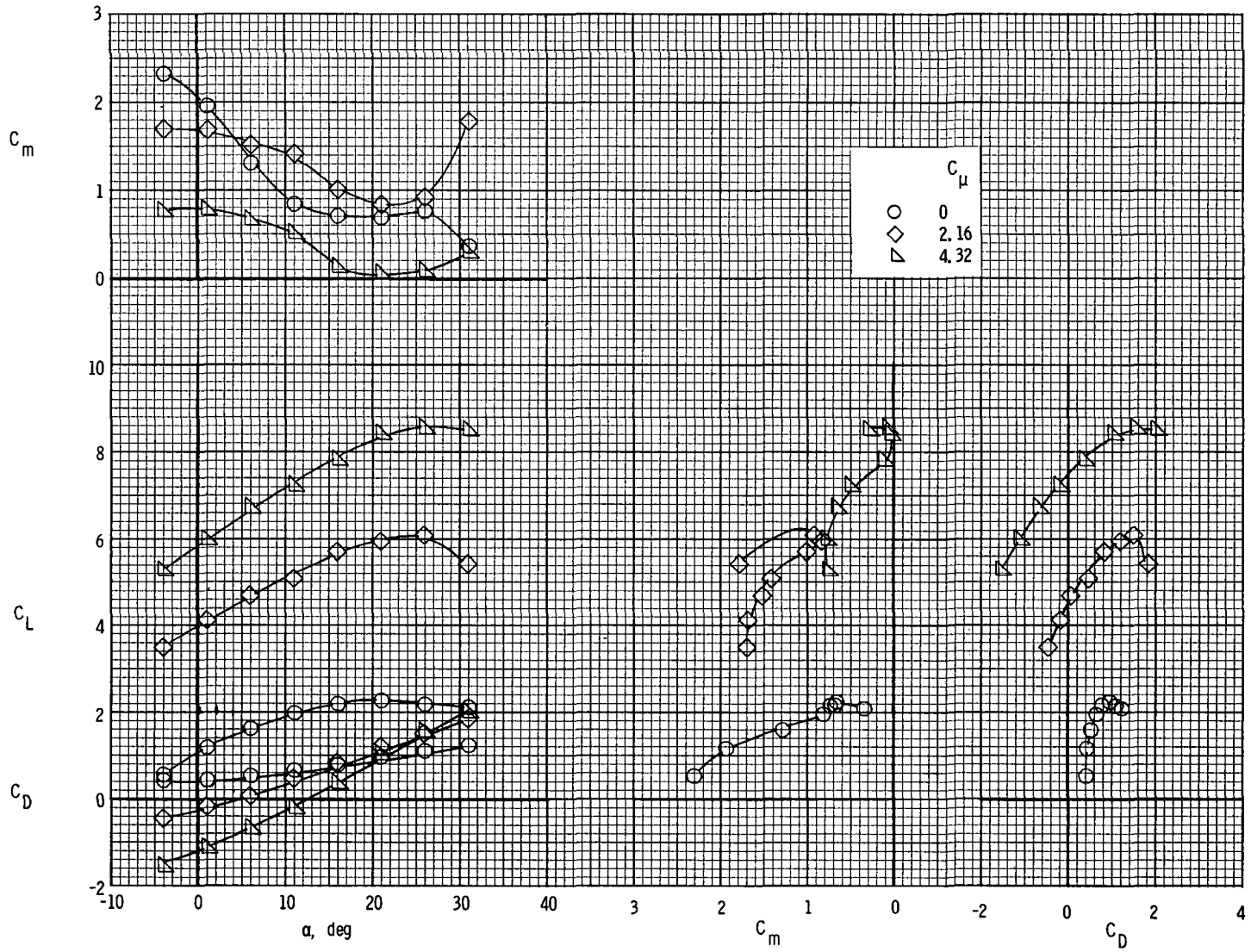
(b)  $\delta_f = 35^\circ$ .

Figure 11.- Lift-drag polars of the model.



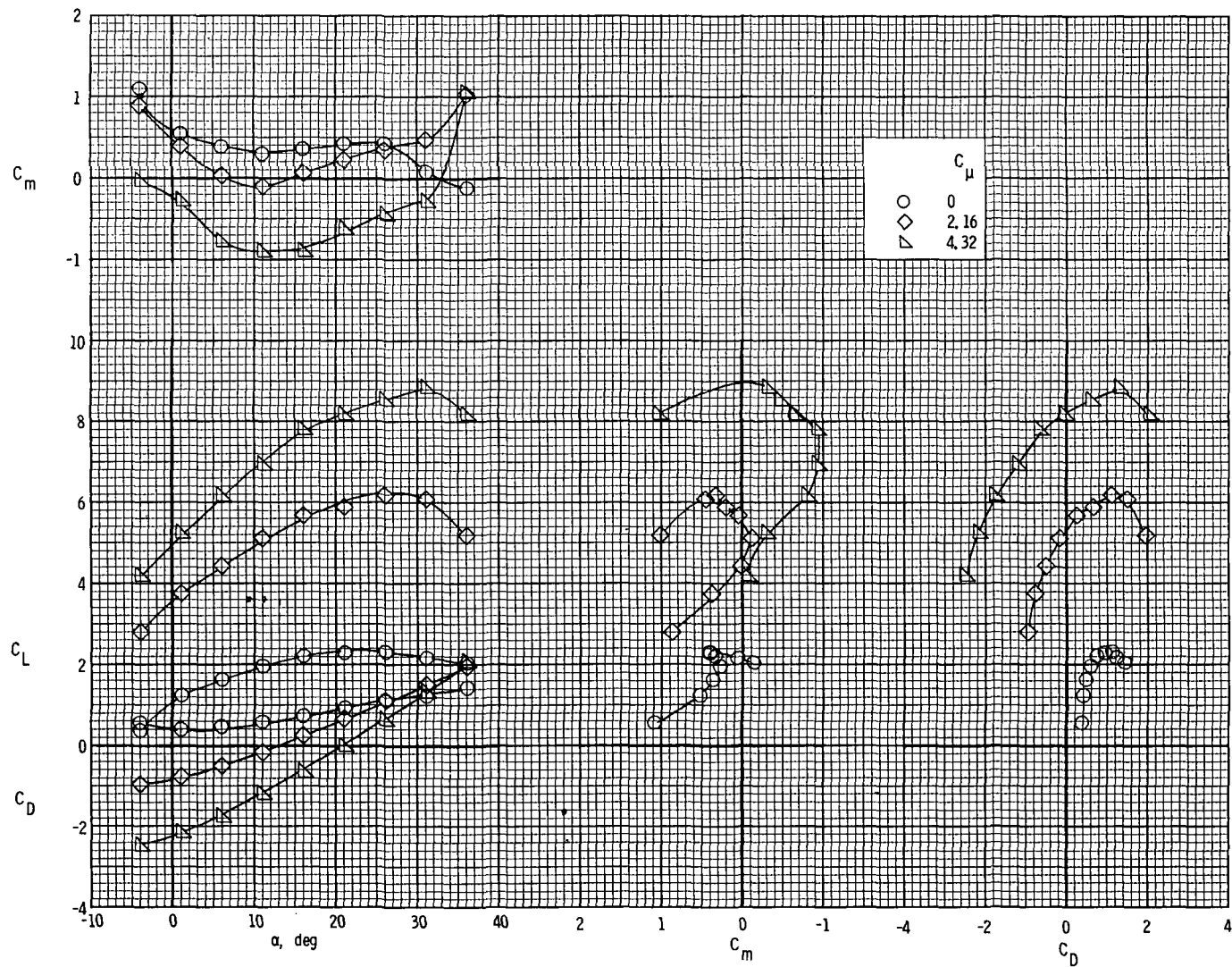
(a)  $i_t = 0^\circ$ .

Figure 12.- Longitudinal characteristics of the model with tail on.  $\delta_f = 55^\circ$ ;  $\delta_e = -40^\circ$ .



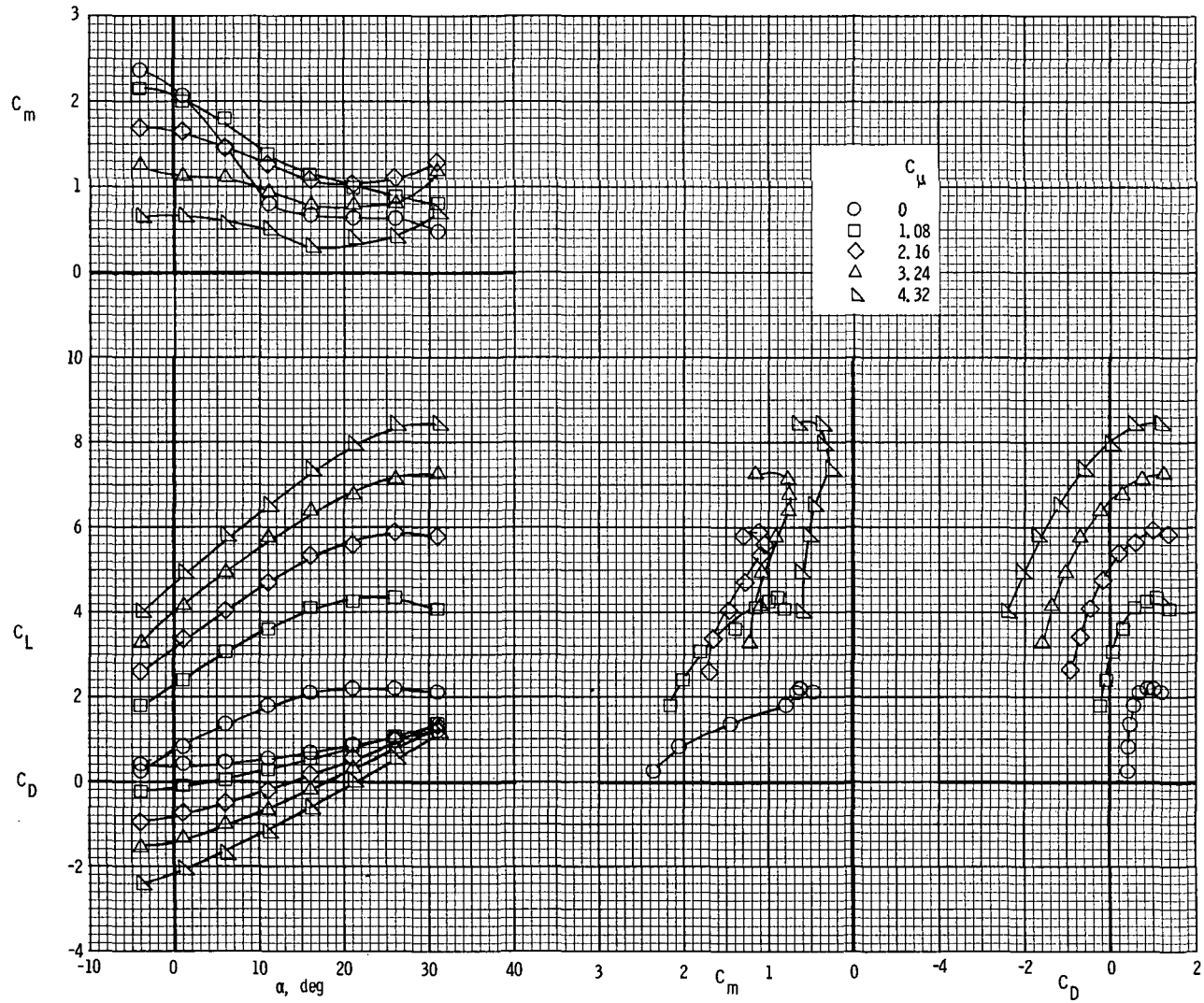
(b)  $i_t = -5^\circ$ .

Figure 12.- Concluded.



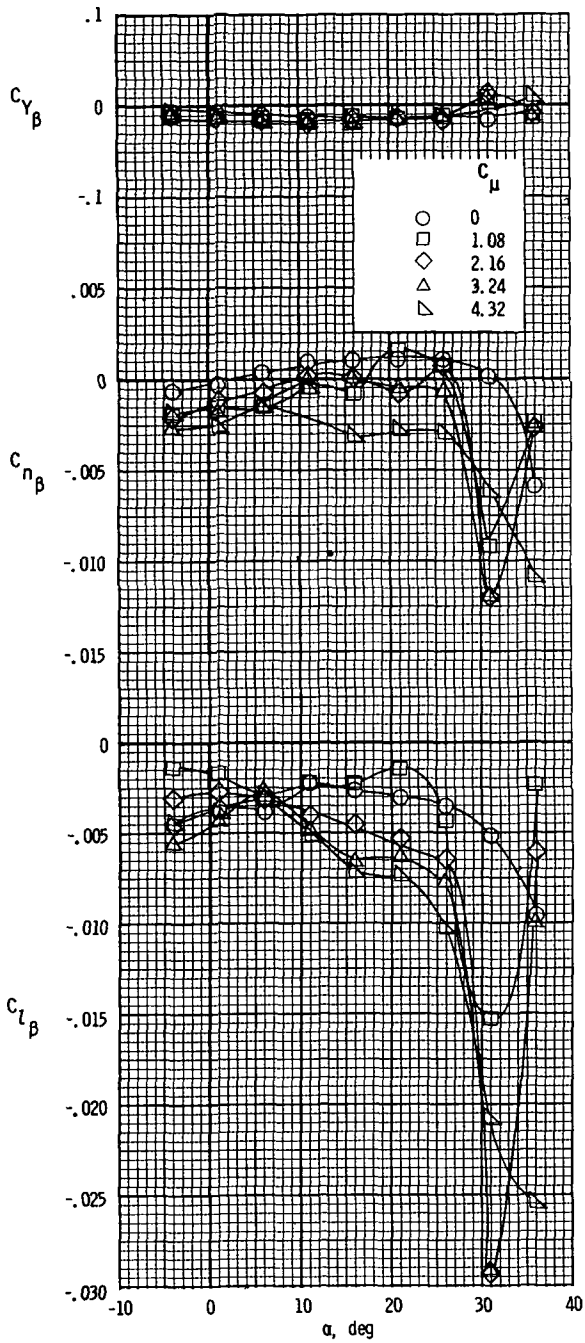
(a)  $i_t = 0^\circ$ .

Figure 13.- Longitudinal characteristics of the model with tail on.  $\delta_f = 35^\circ$ ;  $\delta_e = -40^\circ$ .

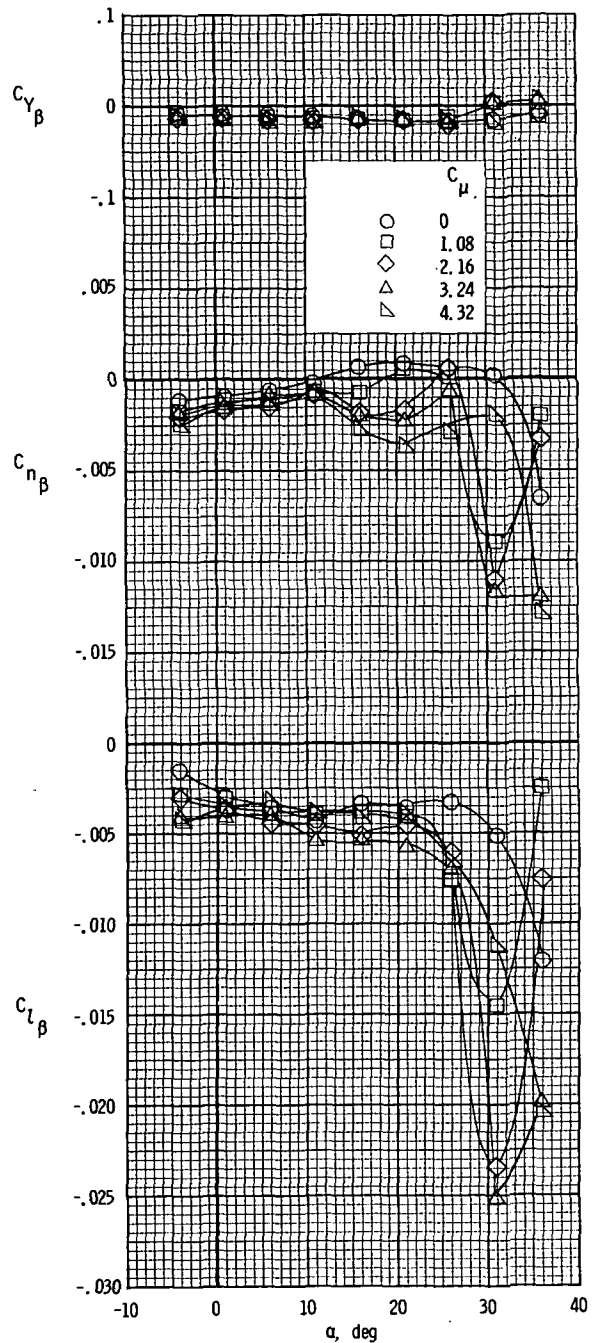


(b)  $i_t = -5^\circ$ .

Figure 13.- Concluded.

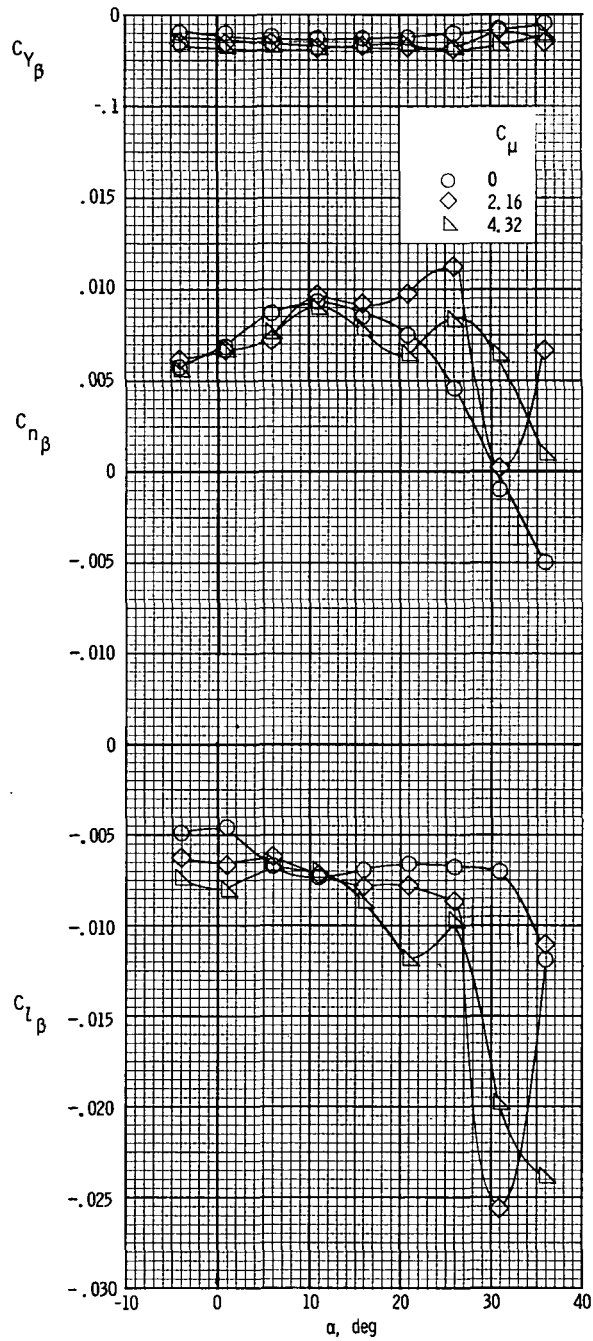


(a)  $\delta_f = 55^\circ$ .

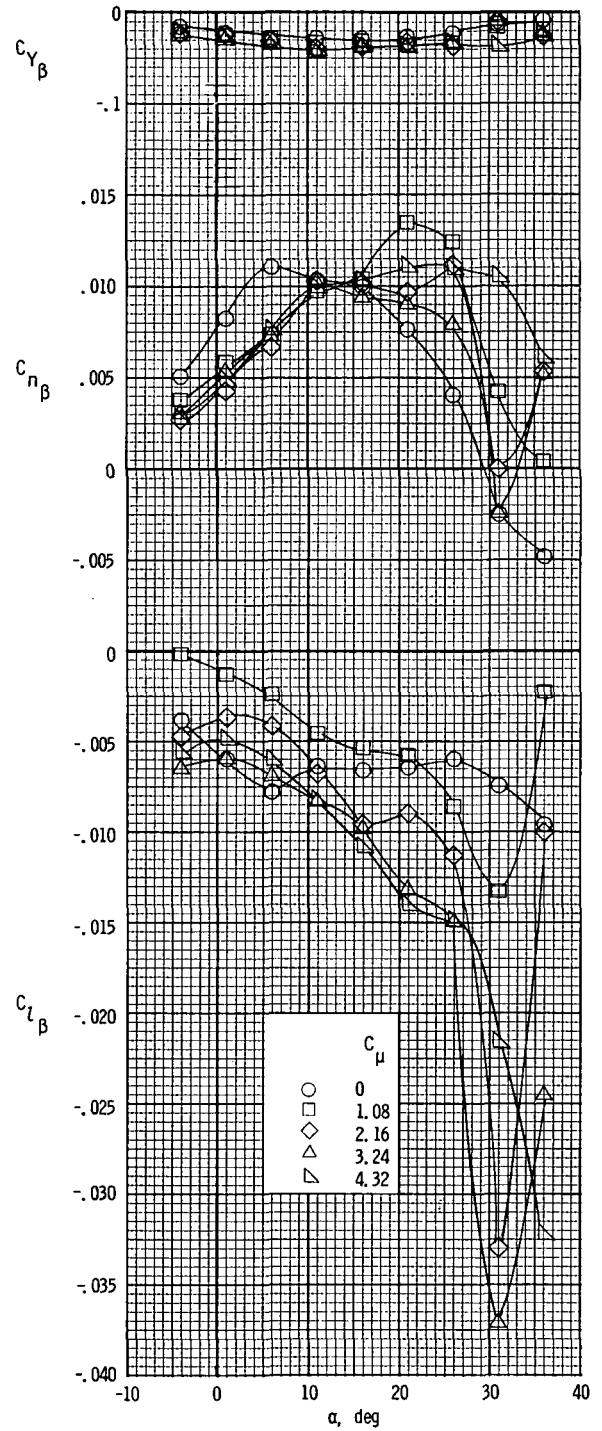


(b)  $\delta_f = 35^\circ$ .

Figure 14.- Static lateral stability characteristics of model with tail off.



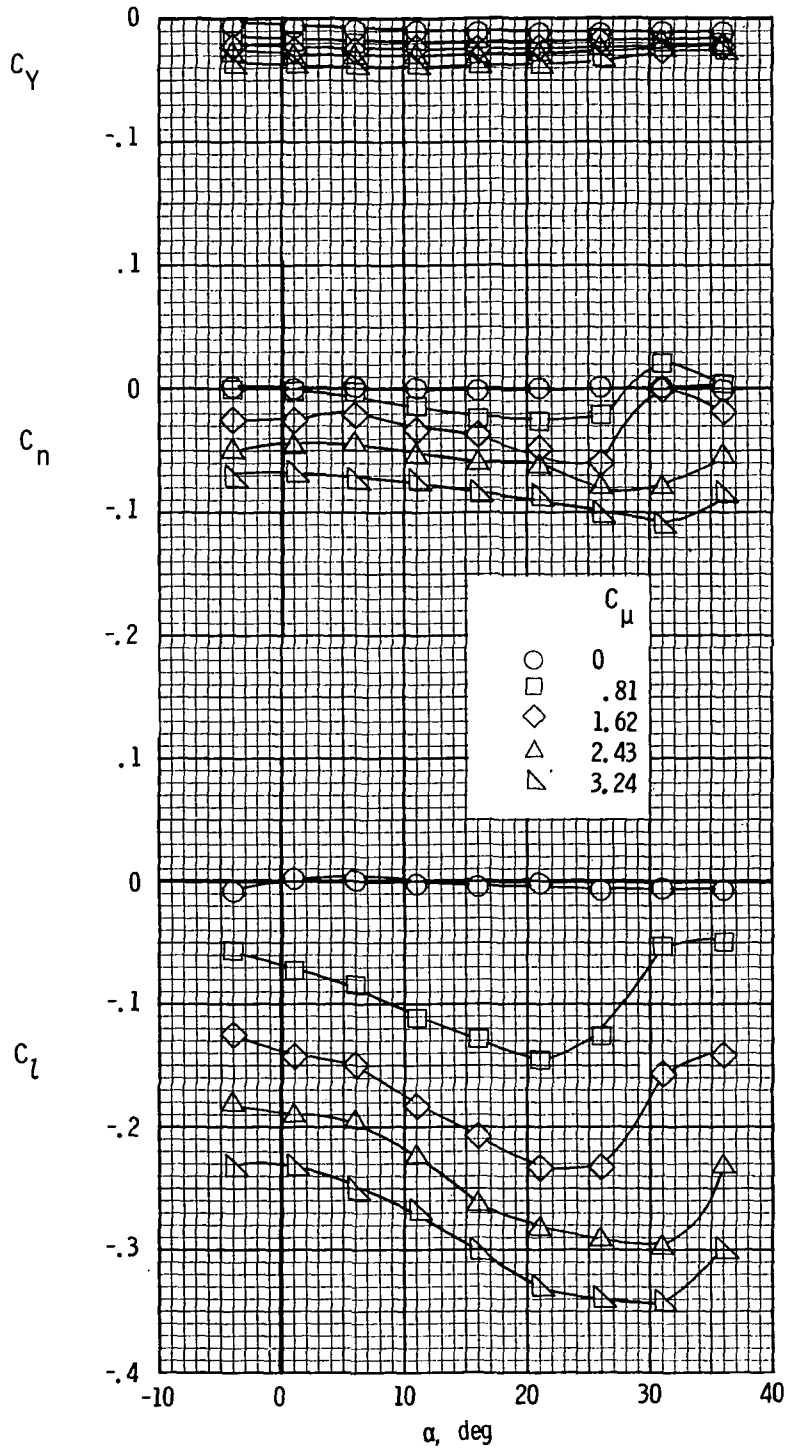
(a)  $\delta_f = 55^\circ$ .



(b)  $\delta_f = 35^\circ$ .

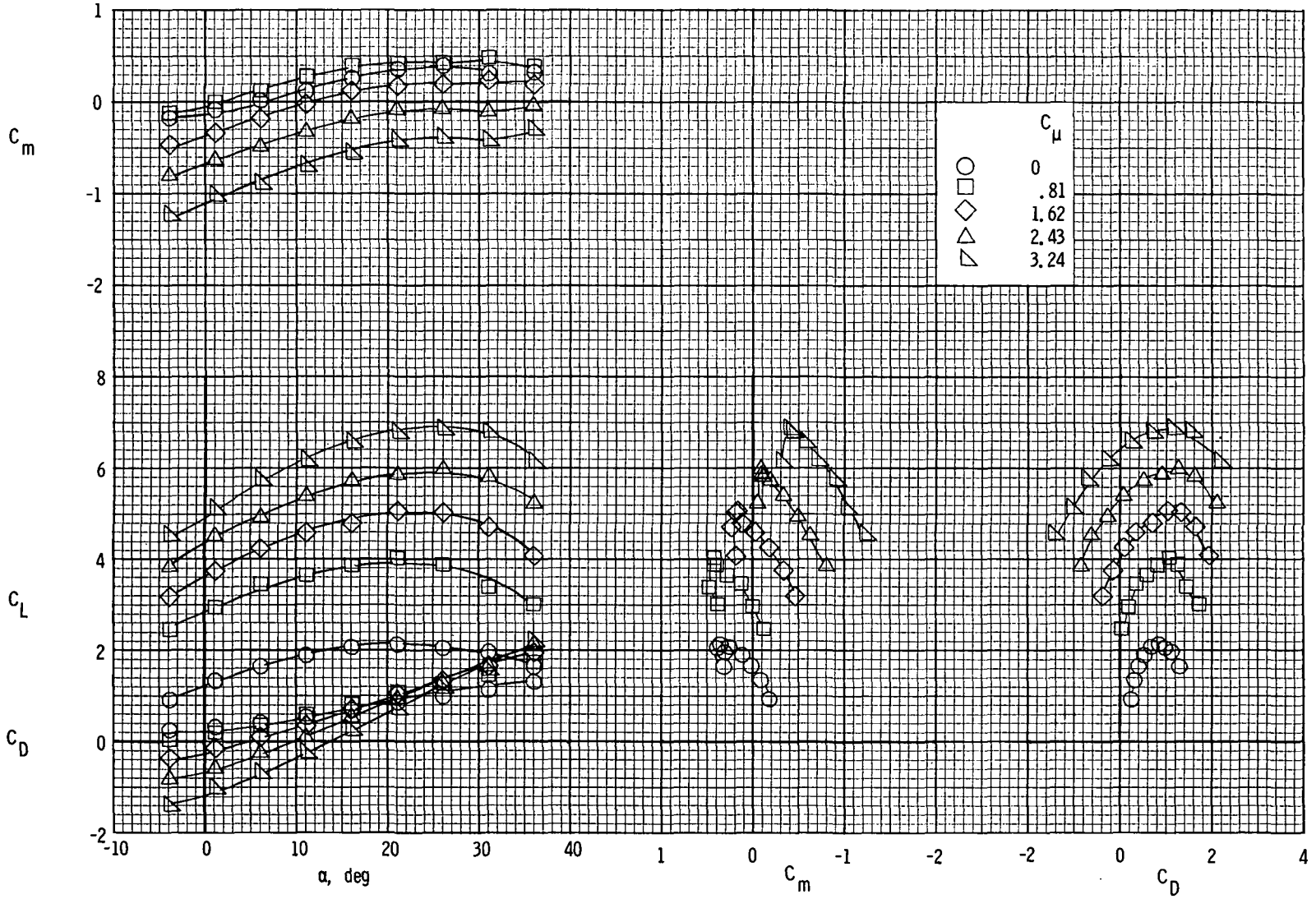
Figure 15.- Static lateral stability characteristics of model with tail on.

$i_t = 0^\circ$ ;  $\delta_e = -40^\circ$ .



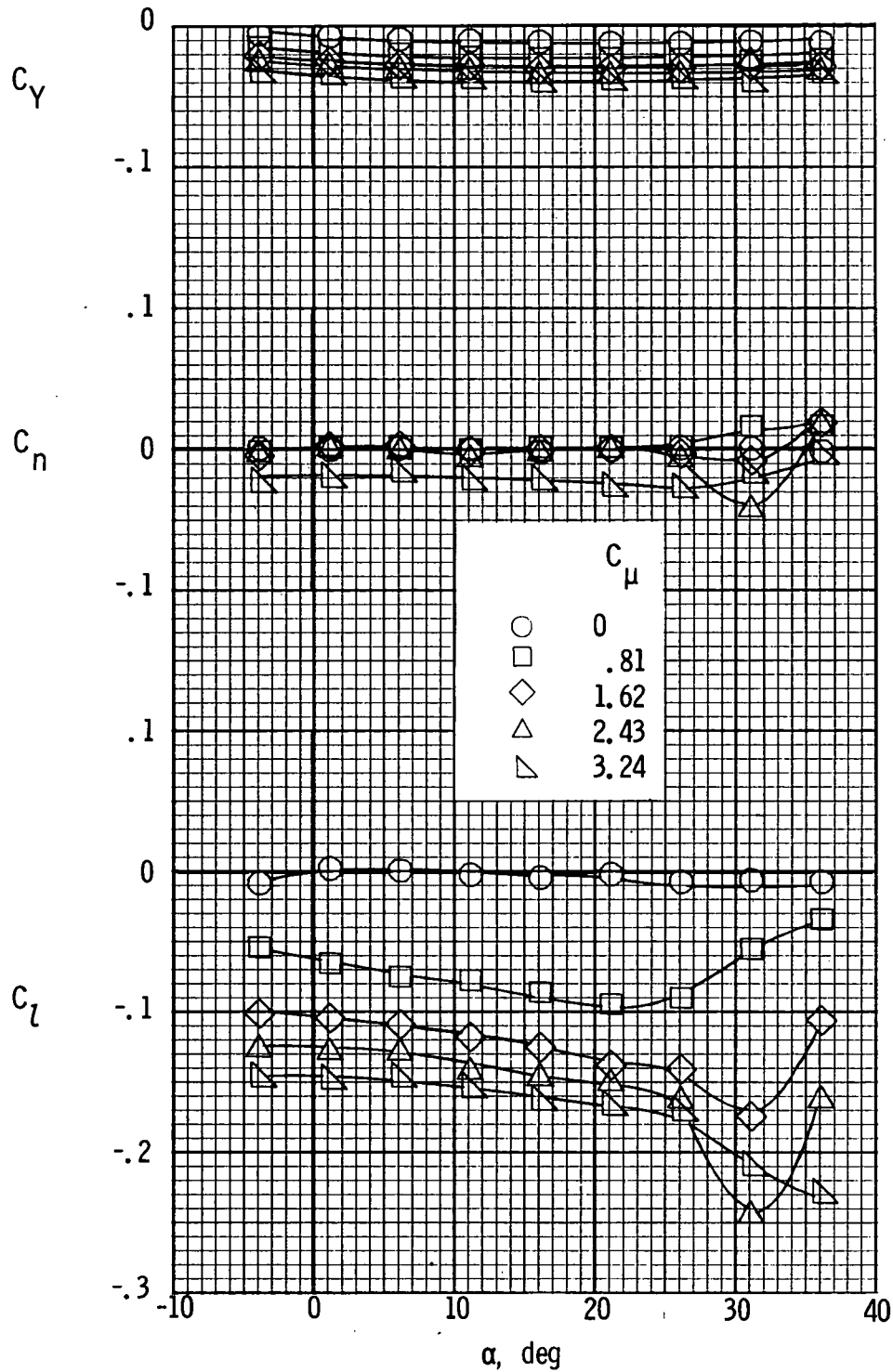
(a) Lateral characteristics.

Figure 16.- Static lateral and longitudinal characteristics of four-engine model with left outboard engine inoperative.  $\delta_f = 55^\circ$ ; tail off; trailing-edge flap slots closed behind engines.



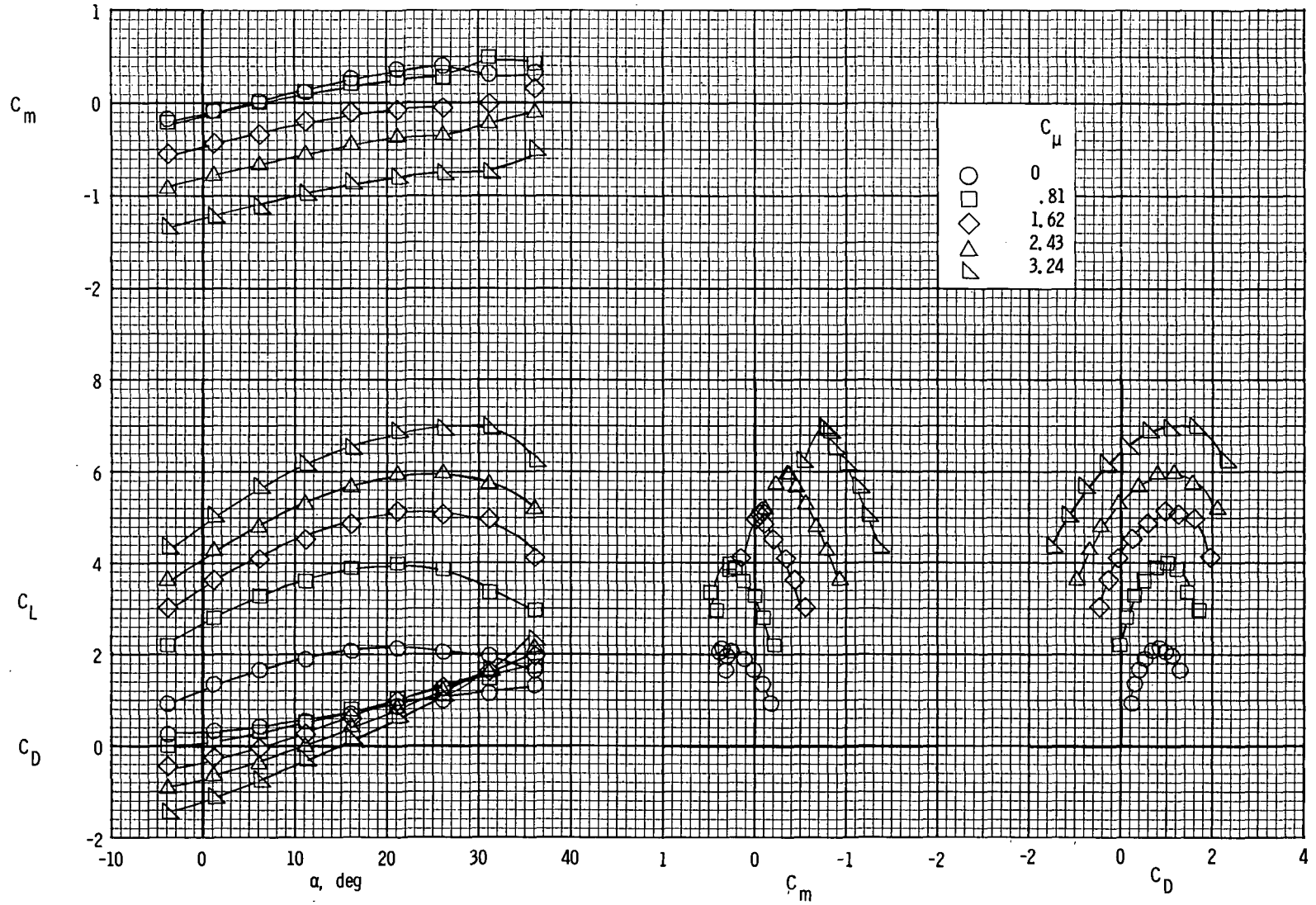
(b) Longitudinal characteristics.

Figure 16.- Concluded.



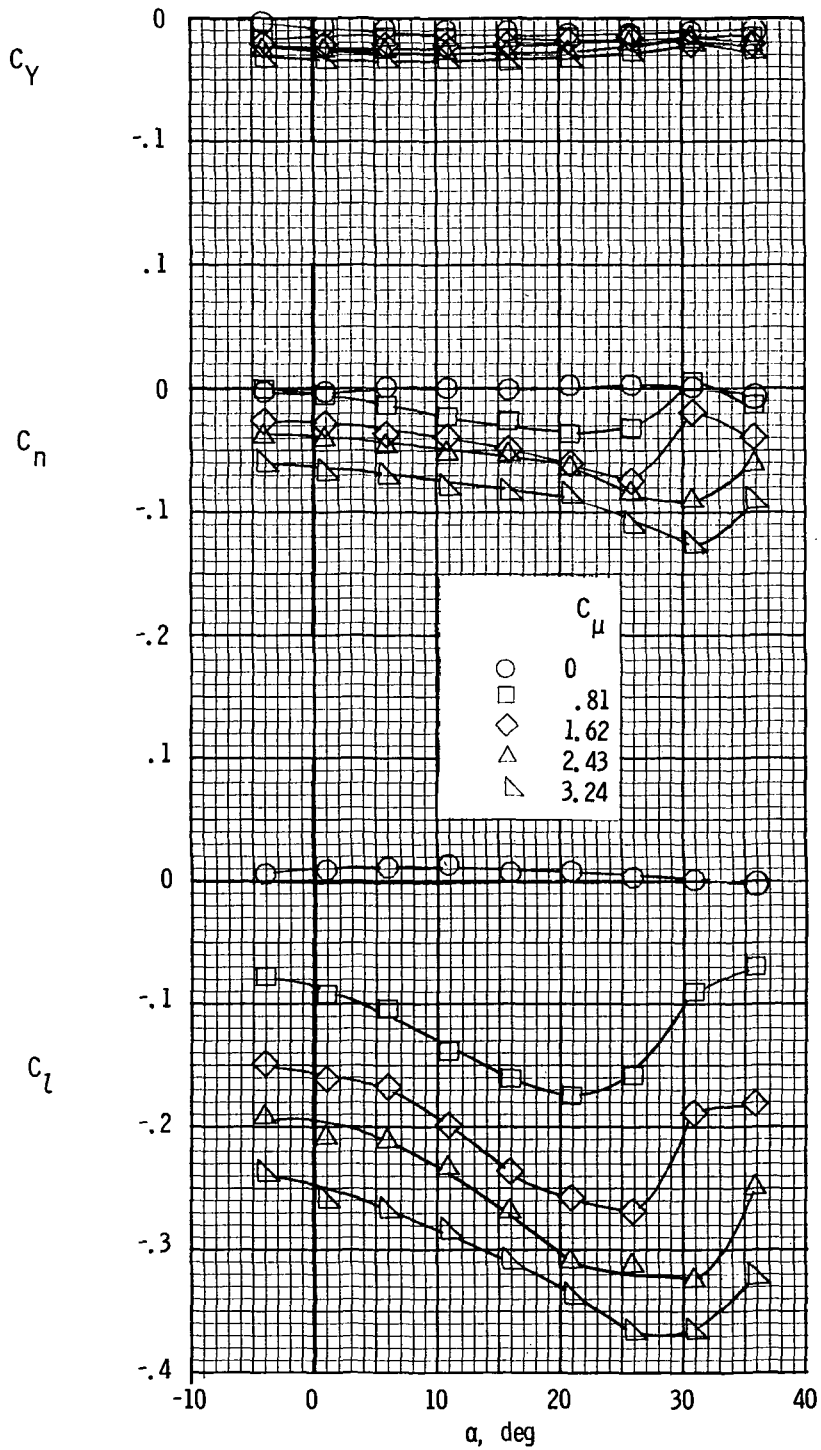
(a) Lateral characteristics.

Figure 17.- Lateral and longitudinal characteristics of four-engine model with left inboard engine inoperative.  $\delta_f = 55^\circ$ ; tail off; trailing-edge flap slots closed behind engines.



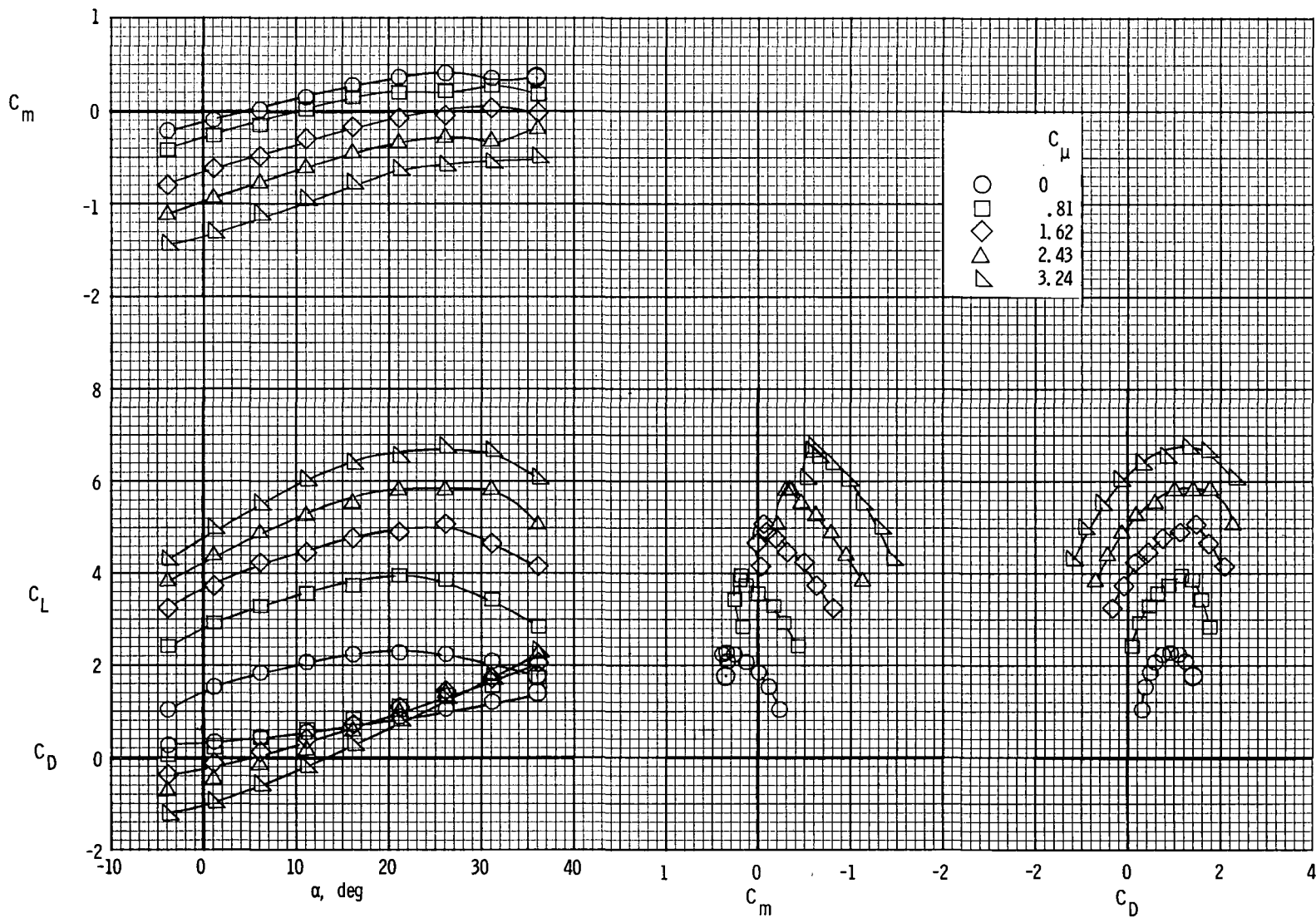
(b) Longitudinal characteristics.

Figure 17.- Concluded.



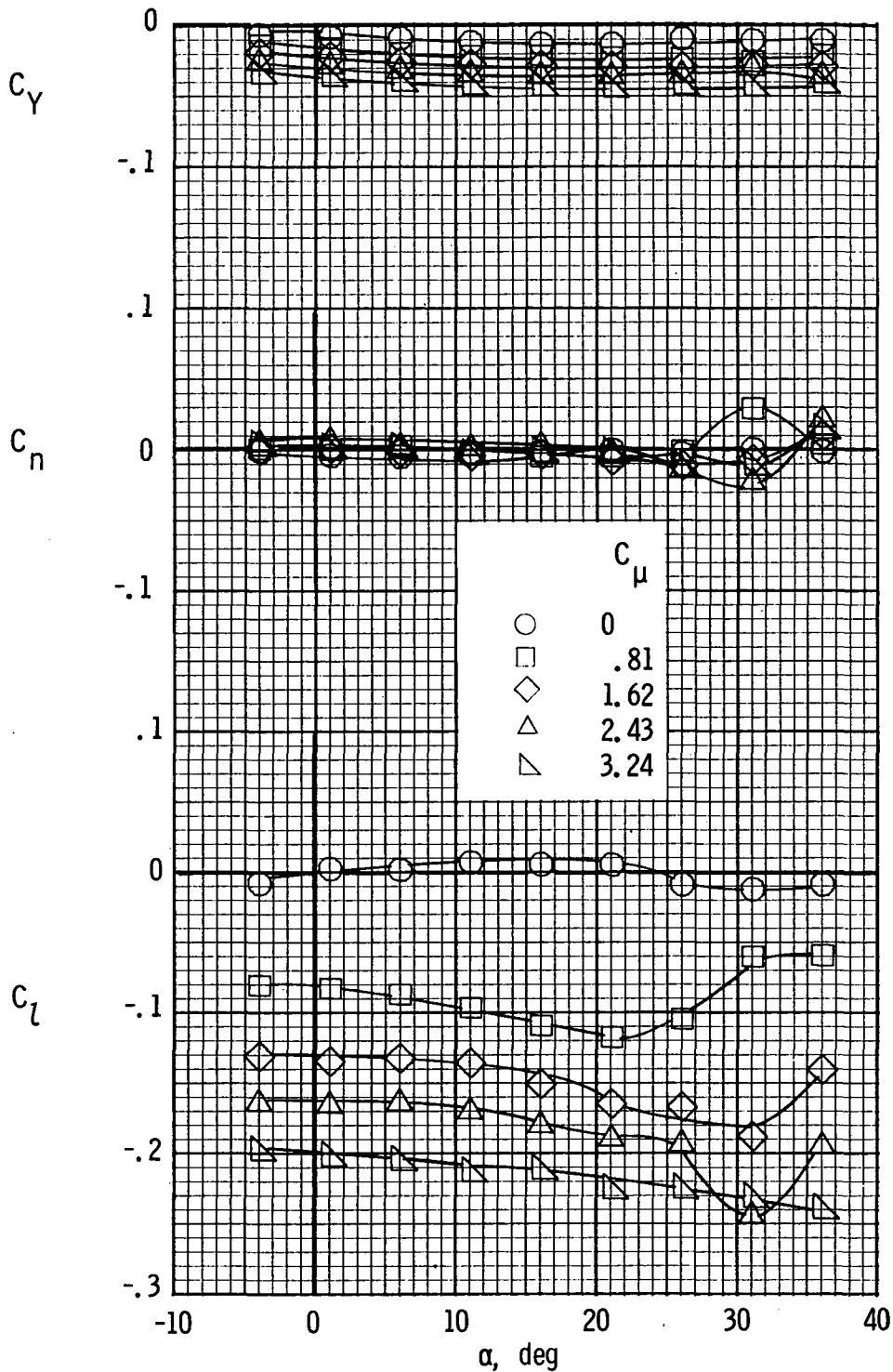
(a) Lateral characteristics.

Figure 18.- Lateral and longitudinal characteristics of four-engine model with left outboard engine inoperative.  $\delta_f = 55^\circ$ ; tail off; trailing-edge flap slots open behind inoperative engine.



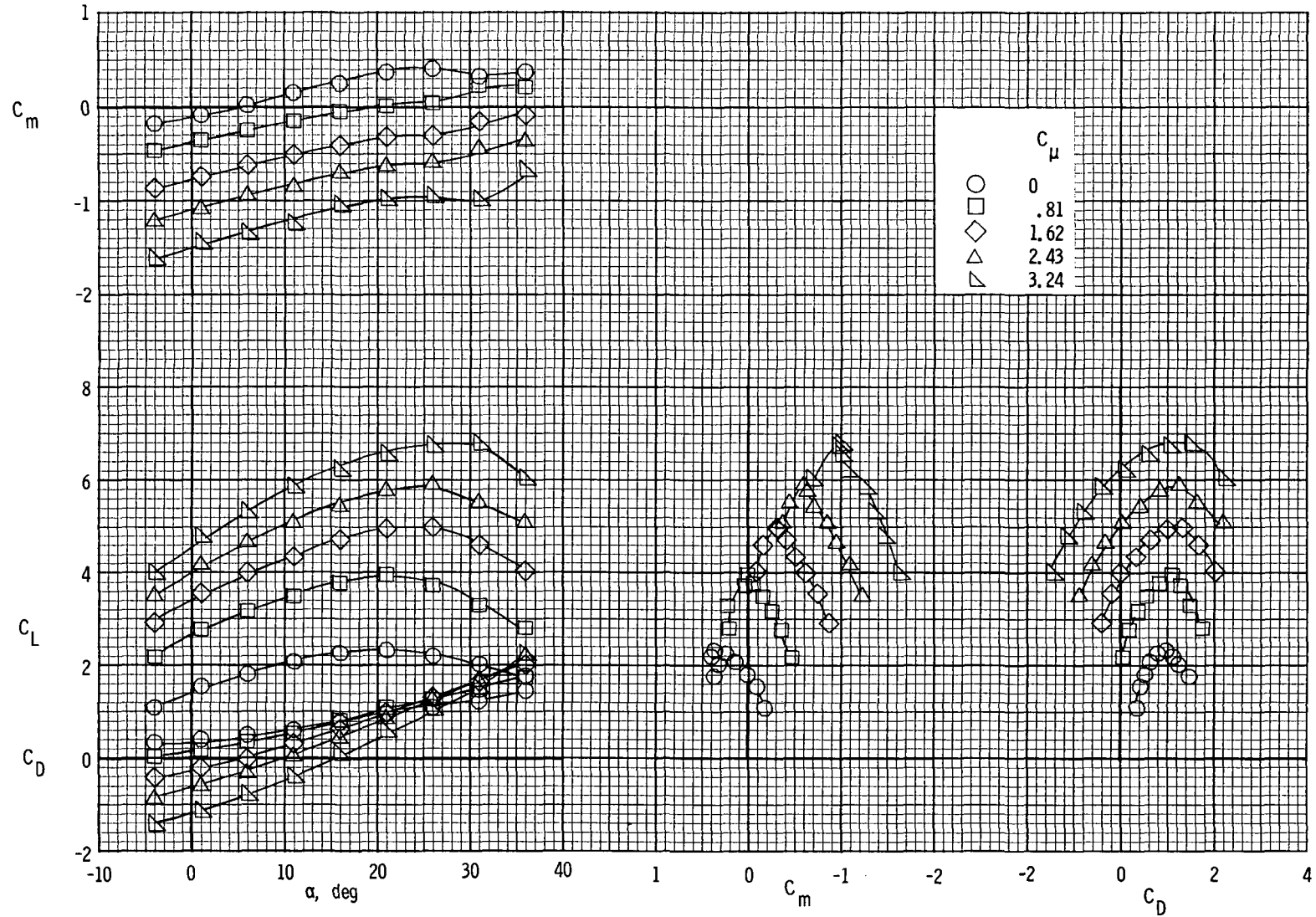
(b) Longitudinal characteristics.

Figure 18.- Concluded.



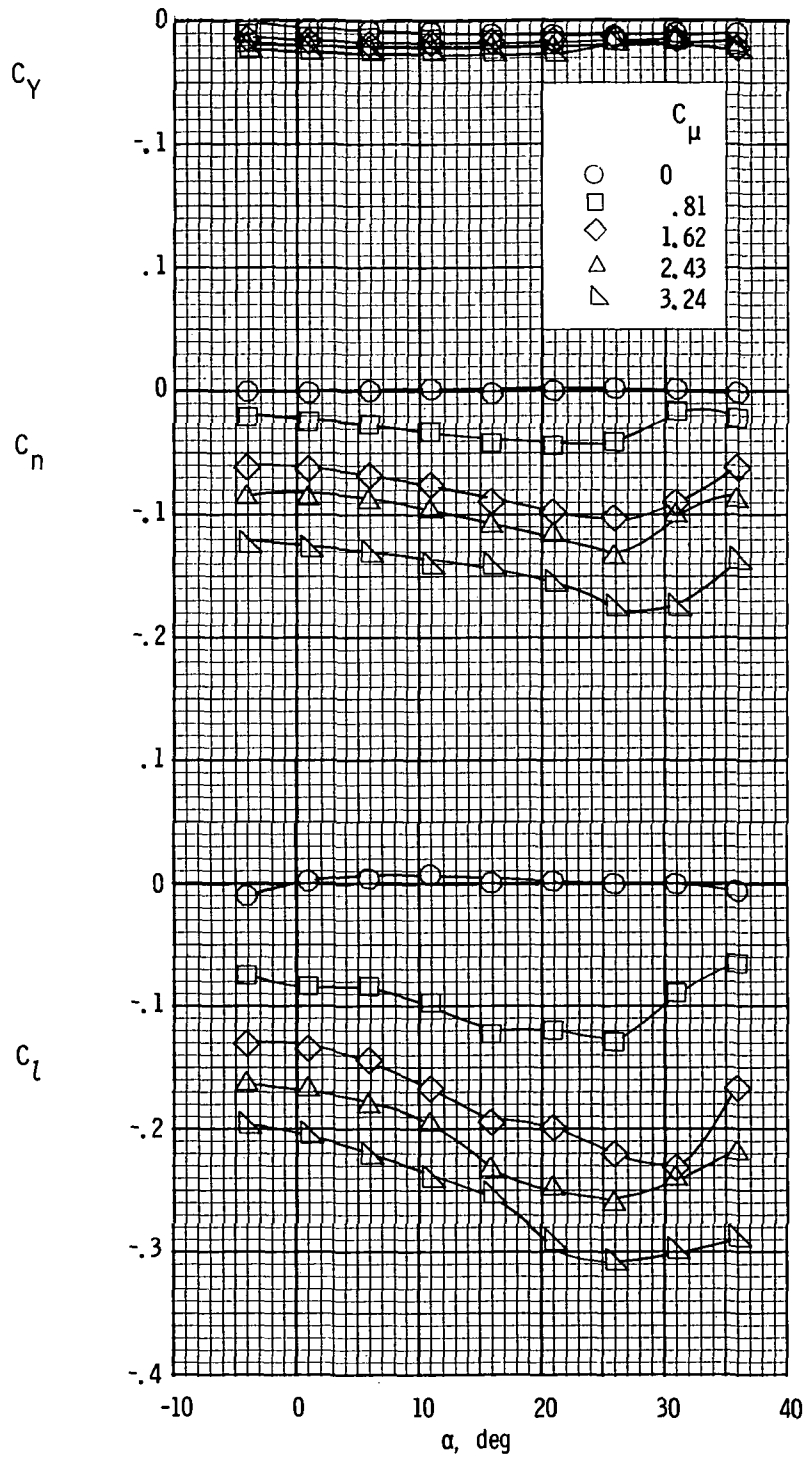
(a) Lateral characteristics.

Figure 19.- Lateral and longitudinal characteristics of four-engine model with left inboard engine inoperative.  $\delta_f = 55^\circ$ ; tail off; trailing-edge flap slots open behind inoperative engine.



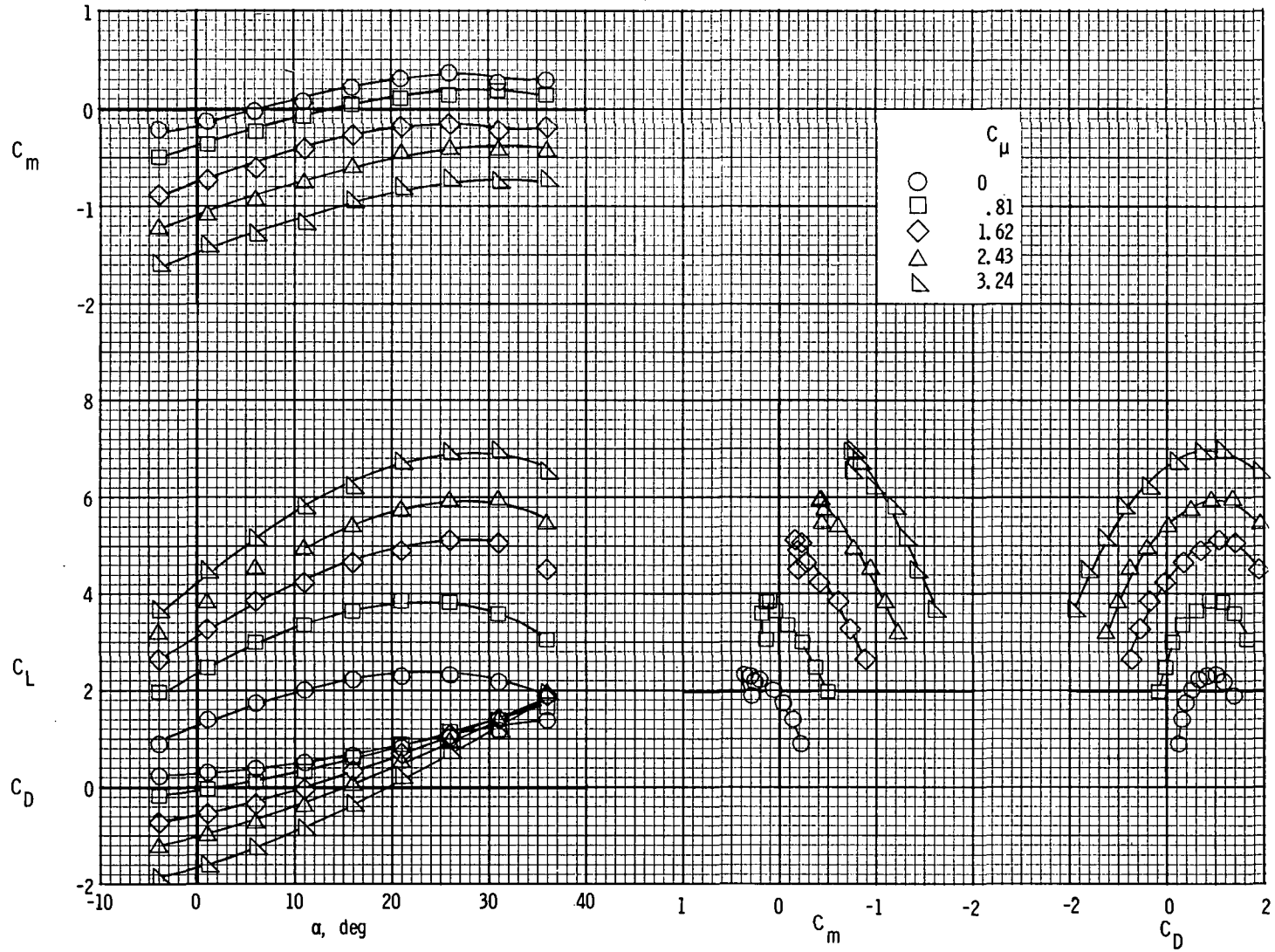
(b) Longitudinal characteristics.

Figure 19.- Concluded.



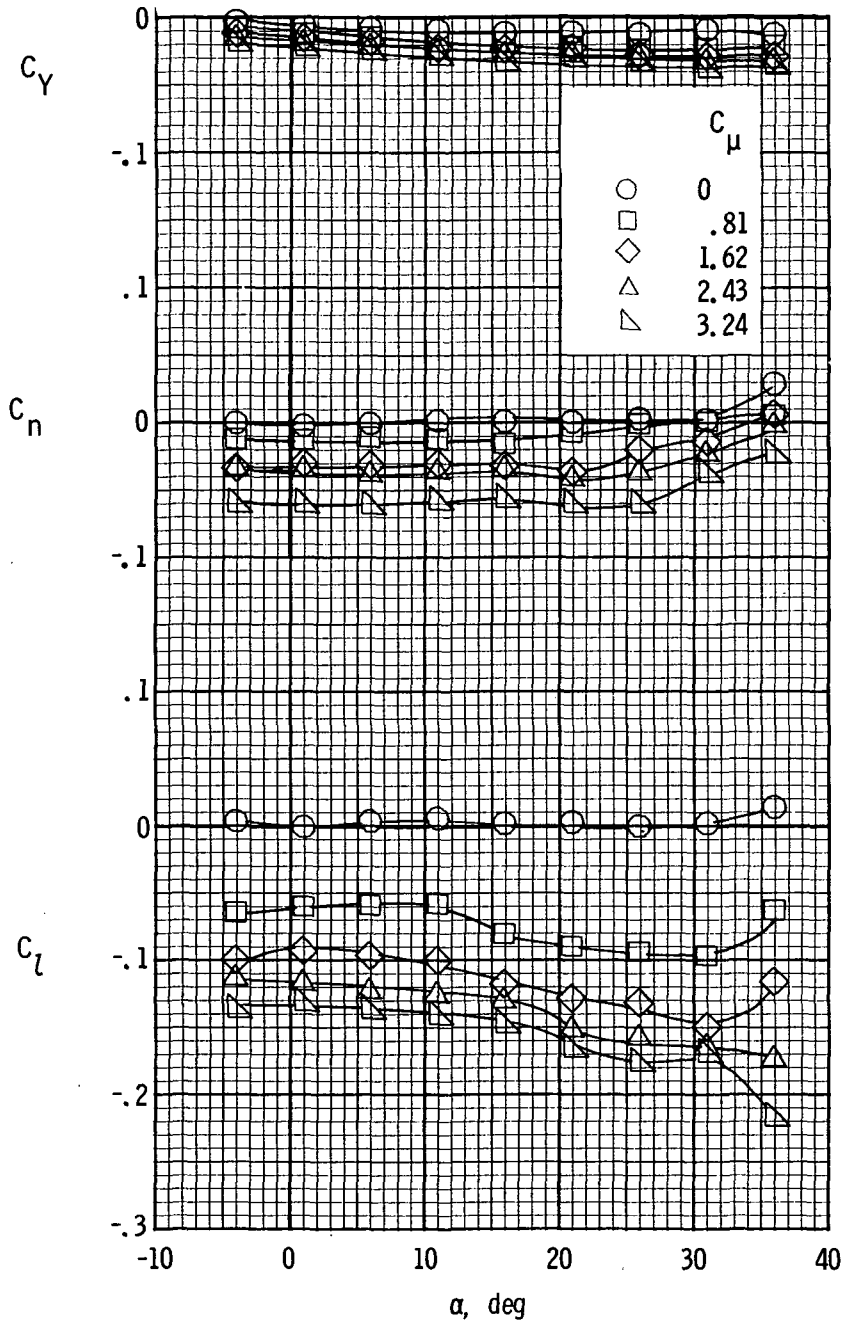
(a) Lateral characteristics.

Figure 20.- Lateral and longitudinal characteristics of four-engine model with left outboard engine inoperative.  $\delta_f = 35^\circ$ ; tail off; trailing-edge flap slots closed behind engines.



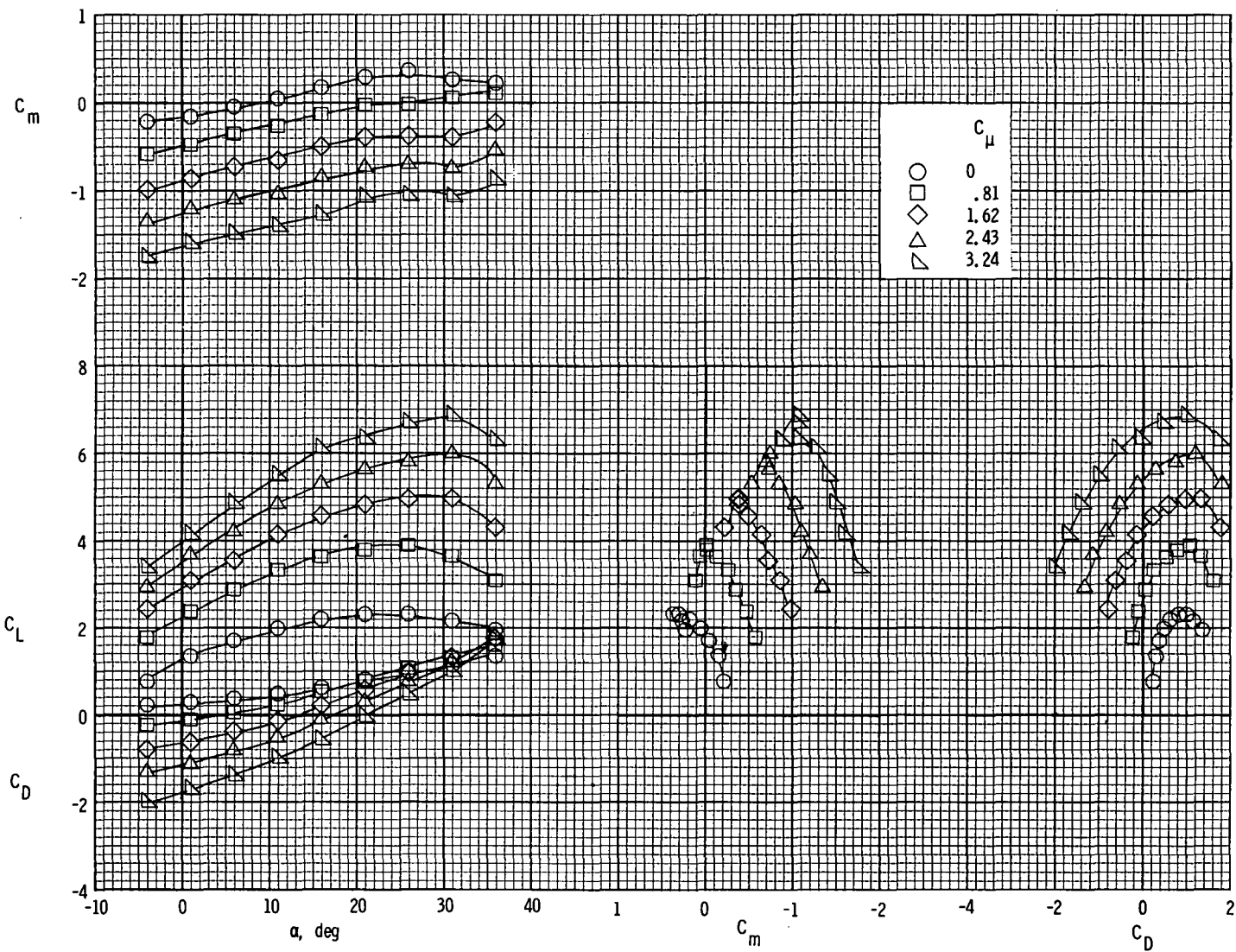
(b) Longitudinal characteristics.

Figure 20.- Concluded.



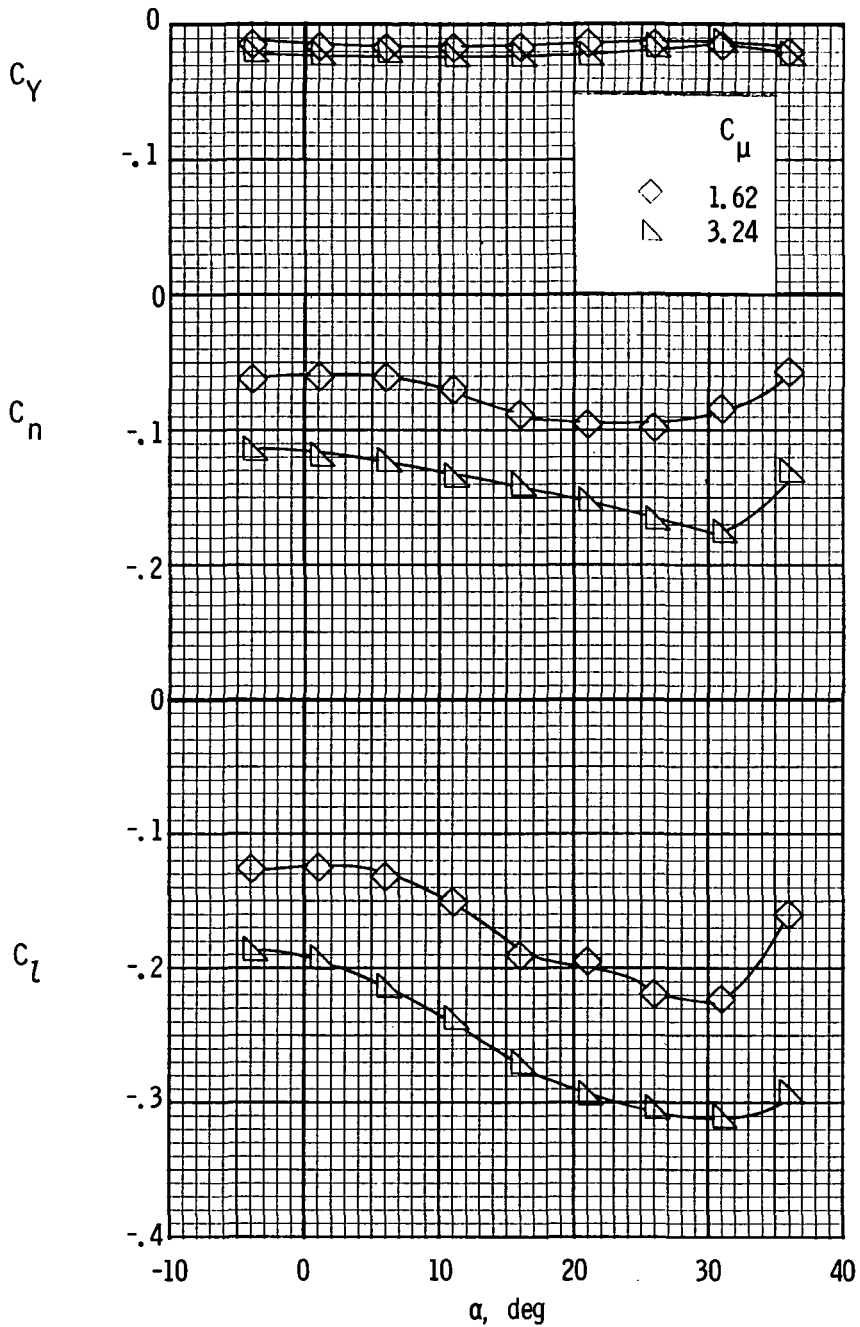
(a) Lateral characteristics.

Figure 21.- Lateral and longitudinal characteristics of four-engine model with left inboard engine inoperative.  $\delta_f = 35^\circ$ ; tail off; trailing-edge flap slots closed behind engines.



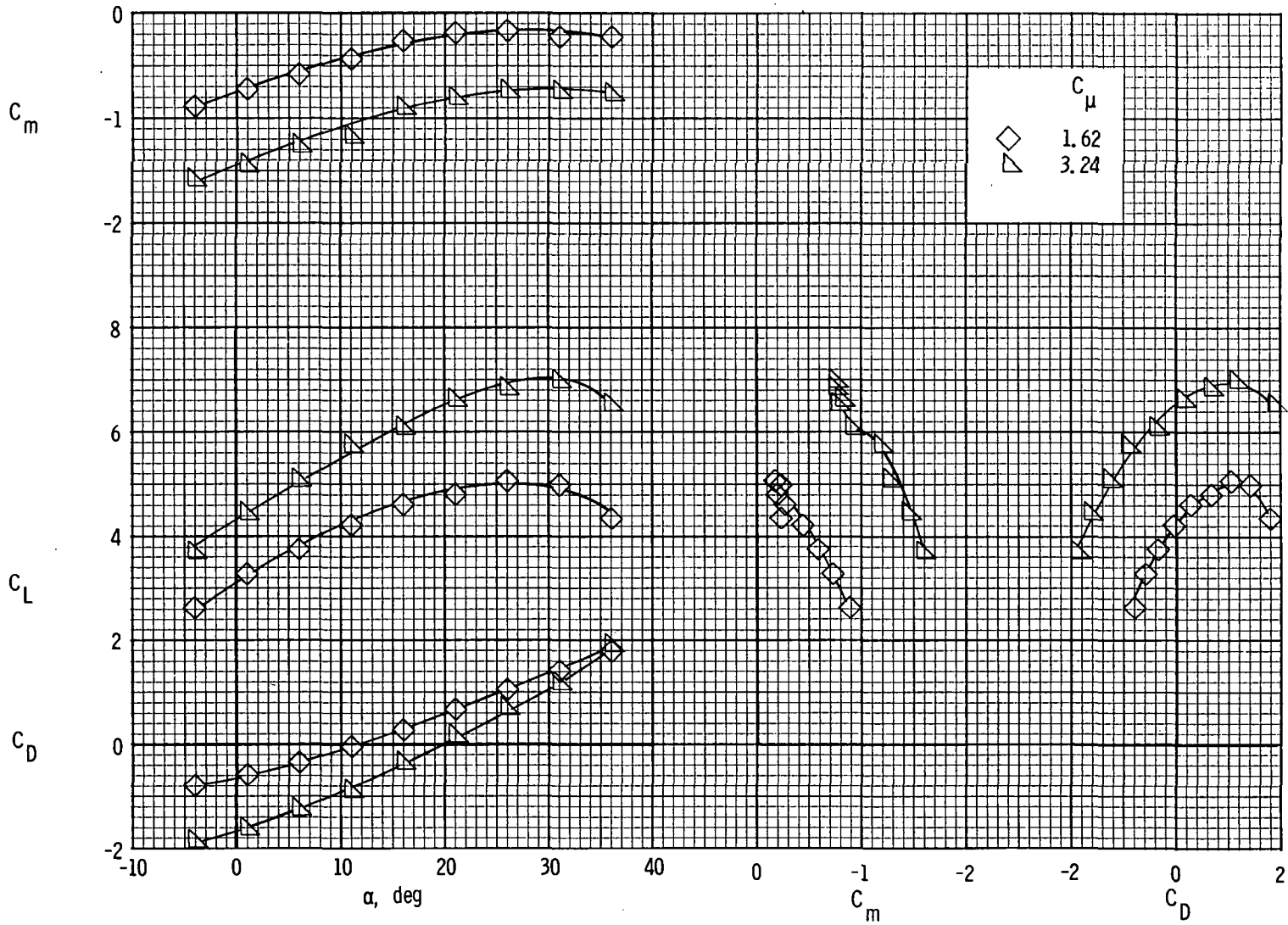
(b) Longitudinal characteristics.

Figure 21.- Concluded.



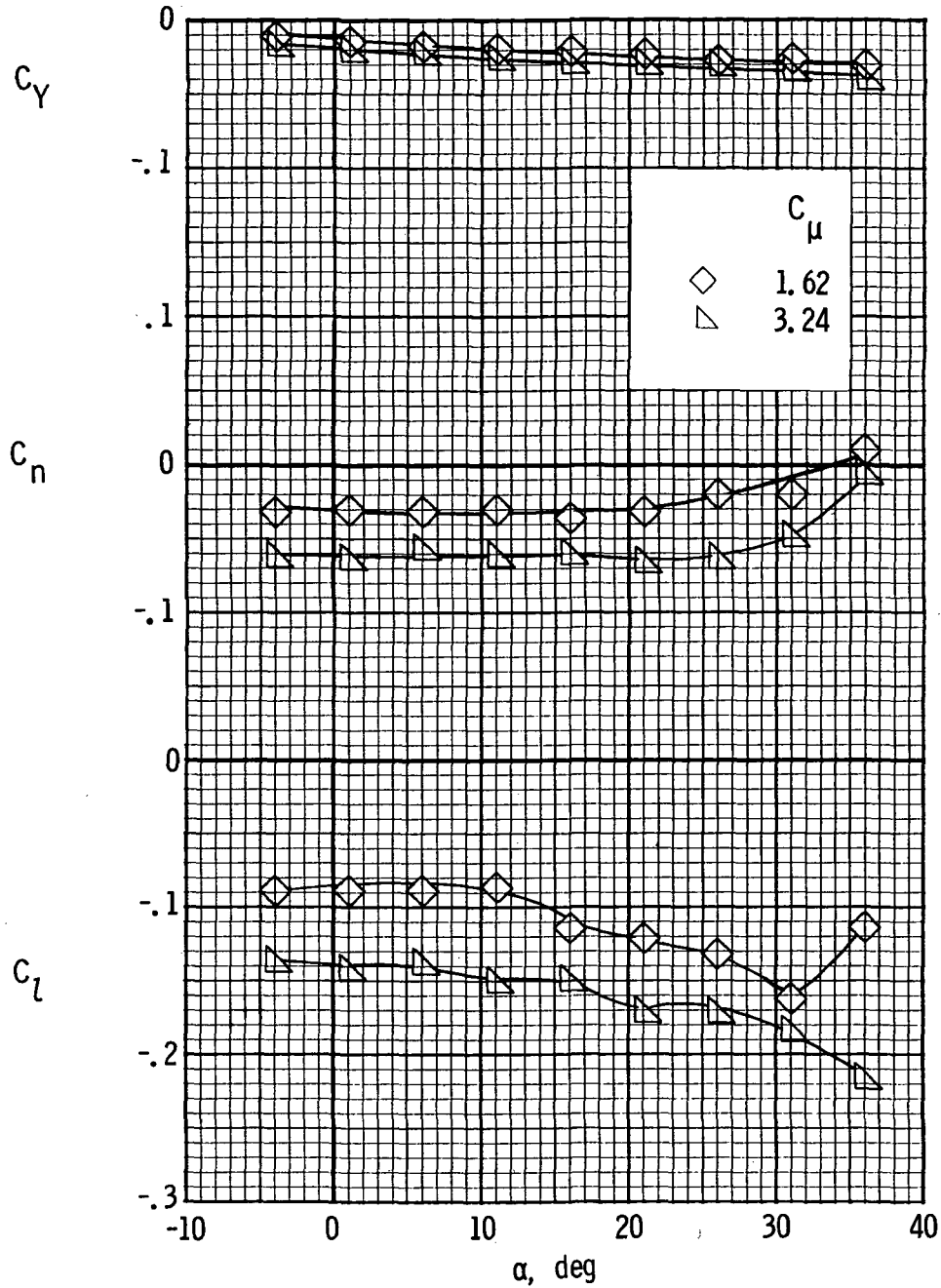
(a) Lateral characteristics.

Figure 22.- Lateral and longitudinal characteristics of four-engine model with left outboard engine inoperative.  $\delta_f = 35^\circ$ ; tail off; trailing-edge flap slots open behind inoperative engine.



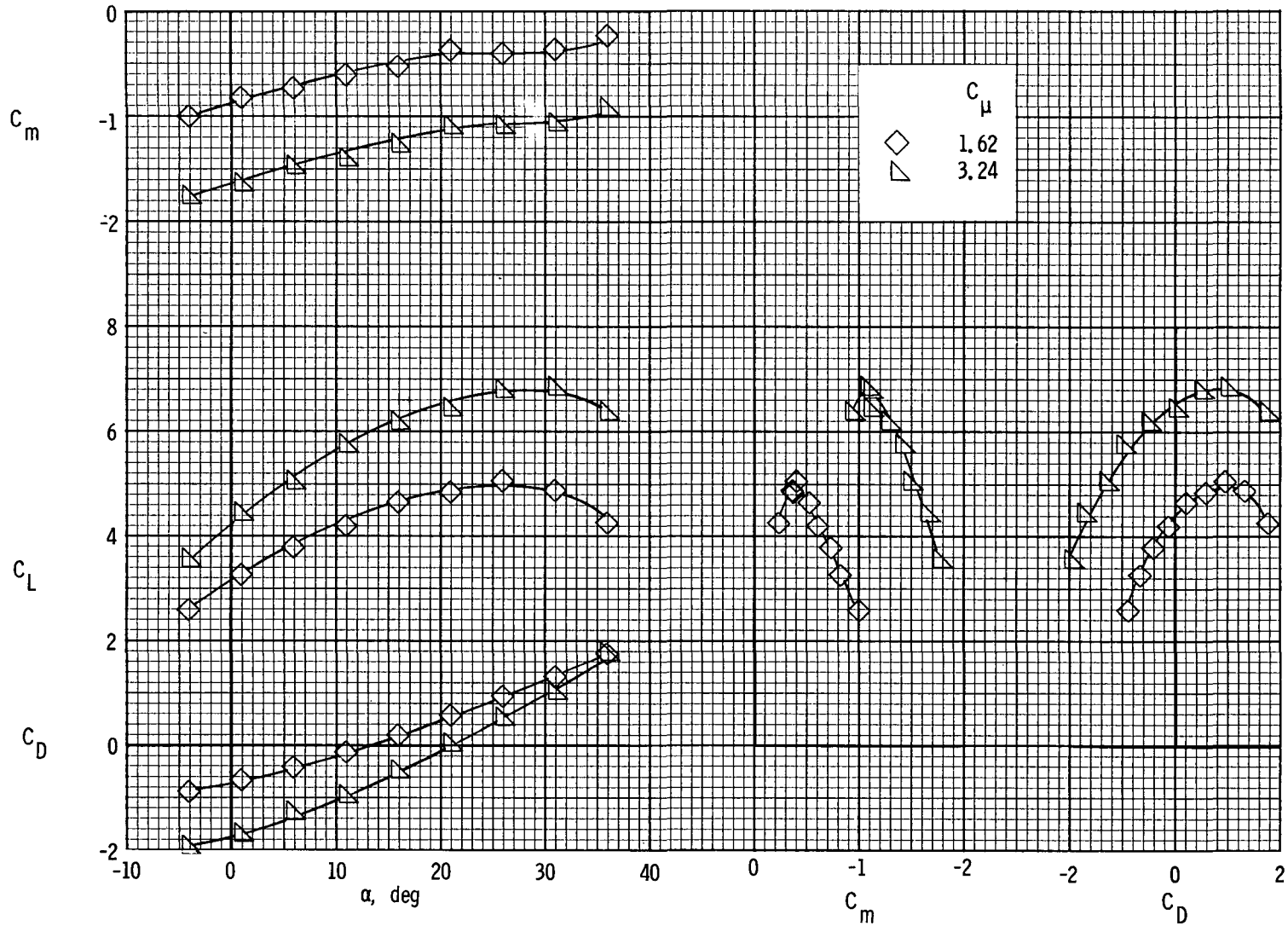
(b) Longitudinal characteristics.

Figure 22.- Concluded.



(a) Lateral characteristics.

Figure 23.- Lateral and longitudinal characteristics of four-engine model with left inboard engine inoperative.  $\delta_f = 35^\circ$ ; tail off; trailing-edge flap slots open behind inoperative engine.



(b) Longitudinal characteristics.

Figure 23.- Concluded.

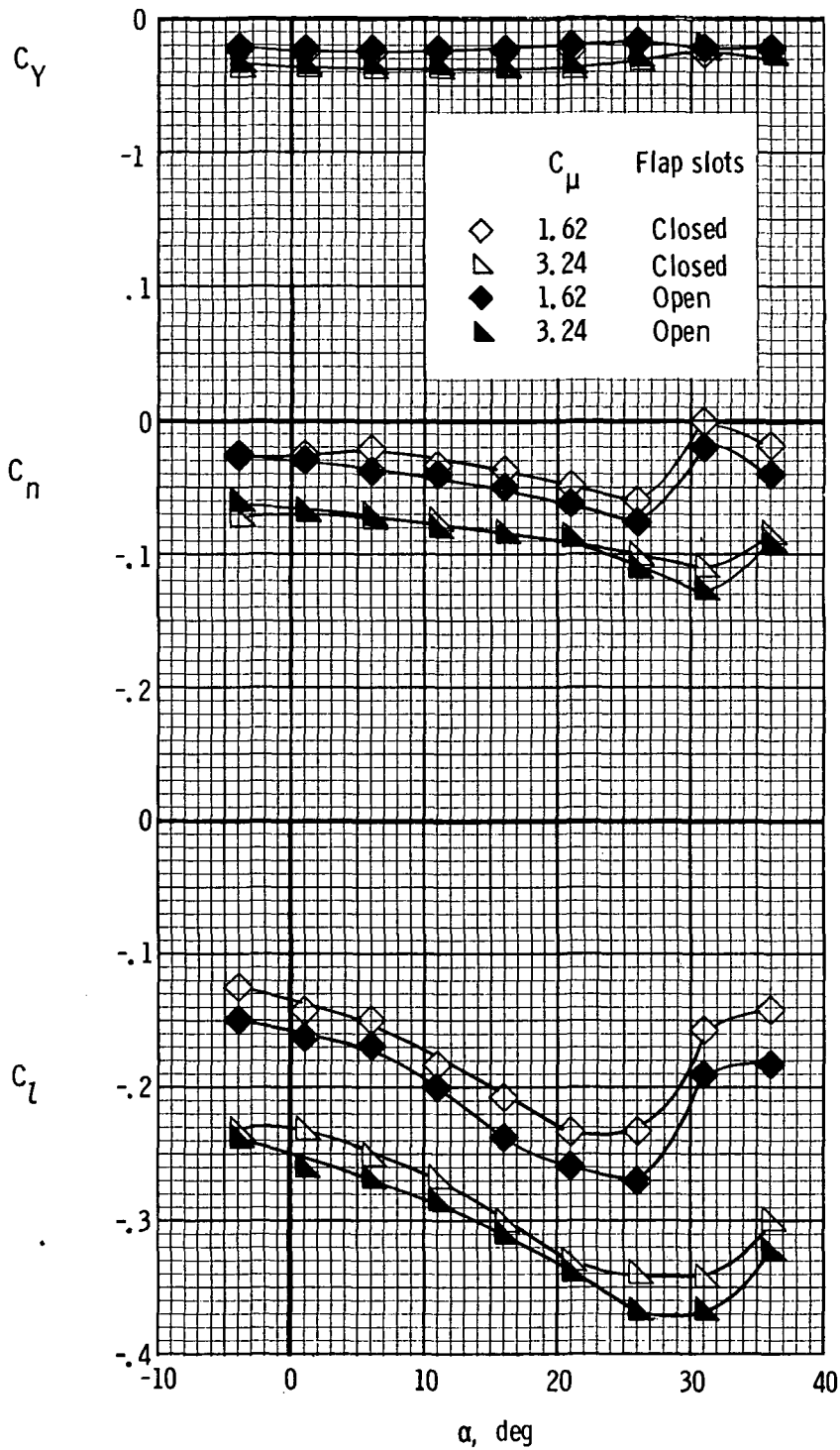
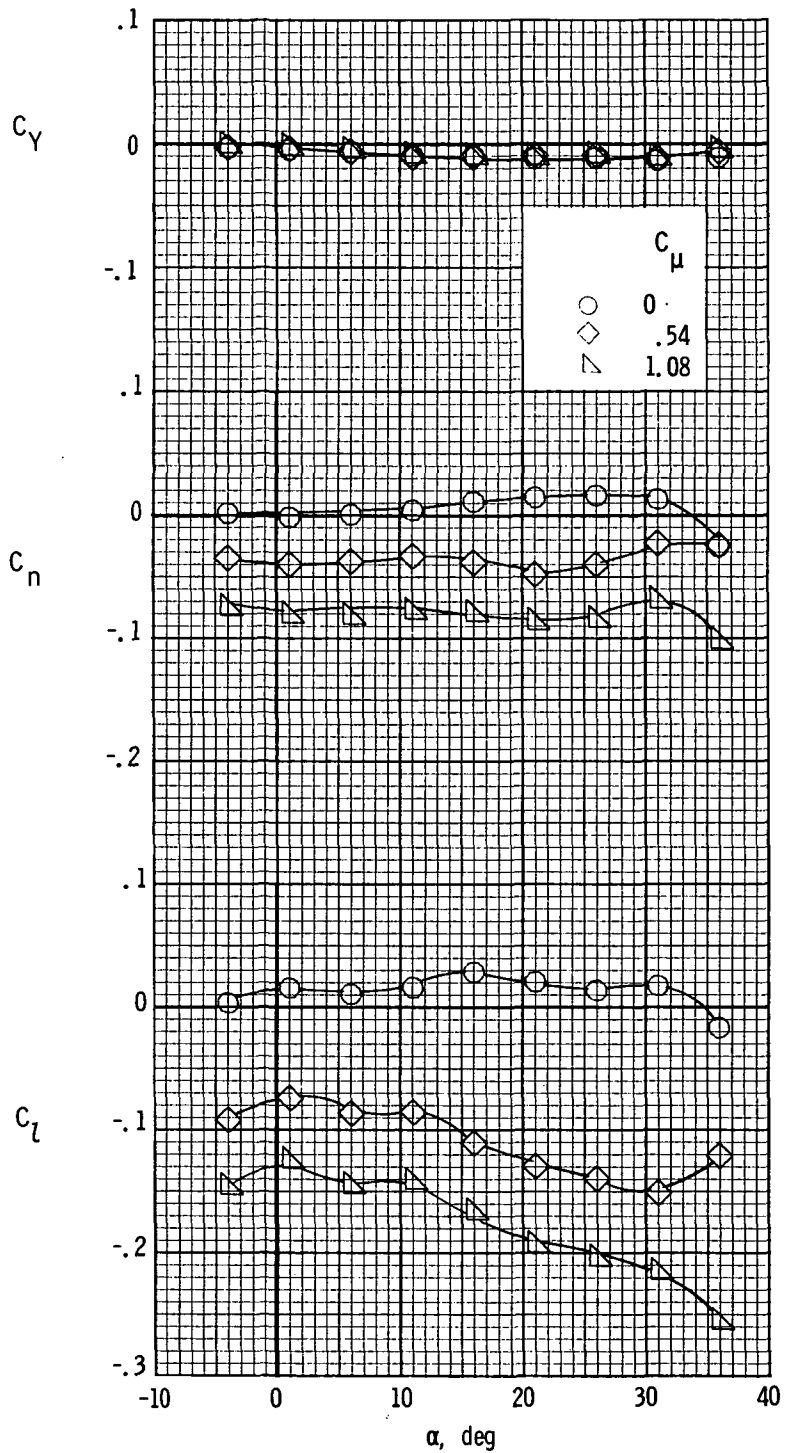
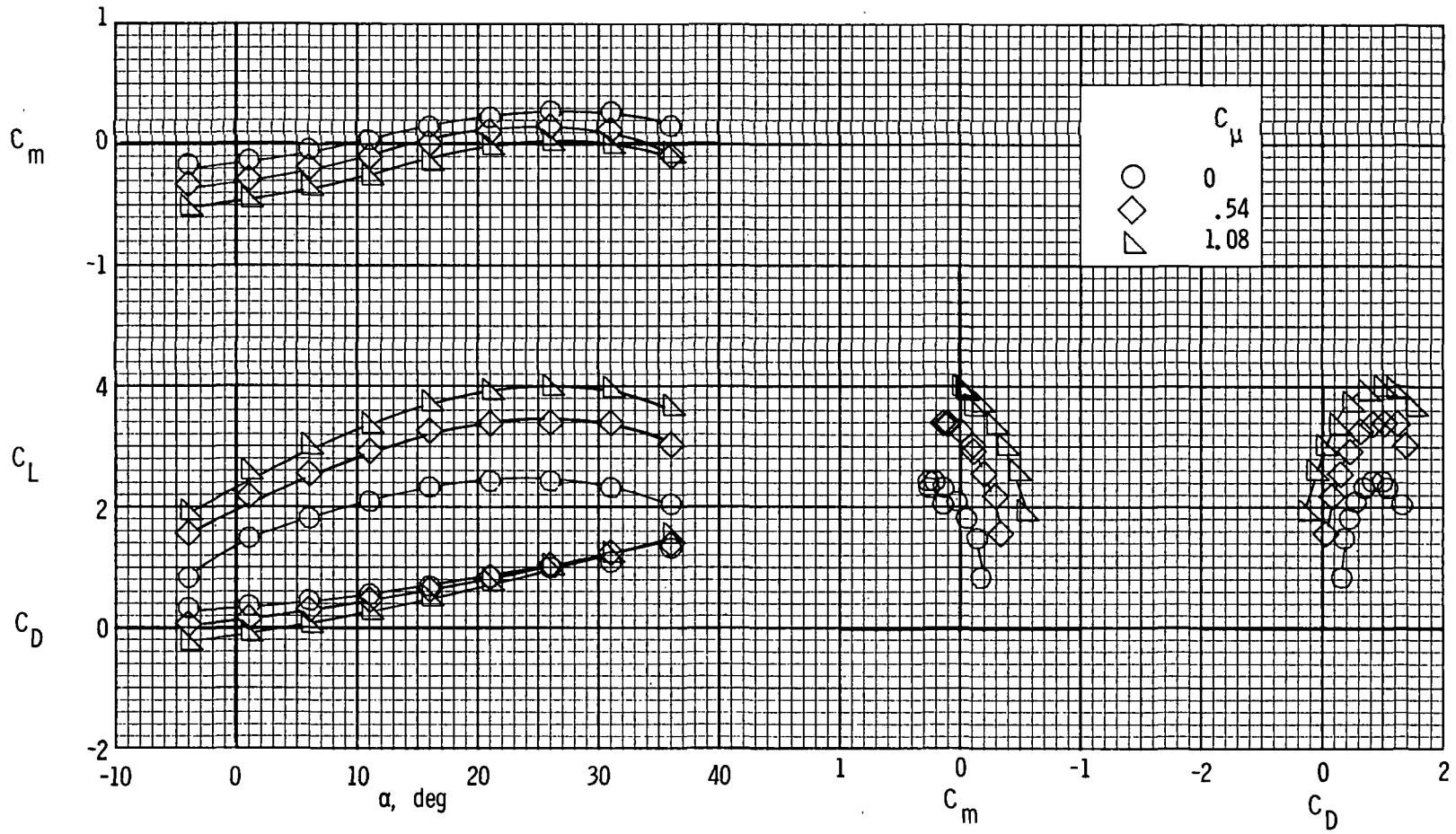


Figure 24.- Effect of closing trailing-edge flap slots behind inoperative engine for four-engine arrangement with left outboard engine inoperative.  $\delta_f = 55^\circ$ ; tail off.



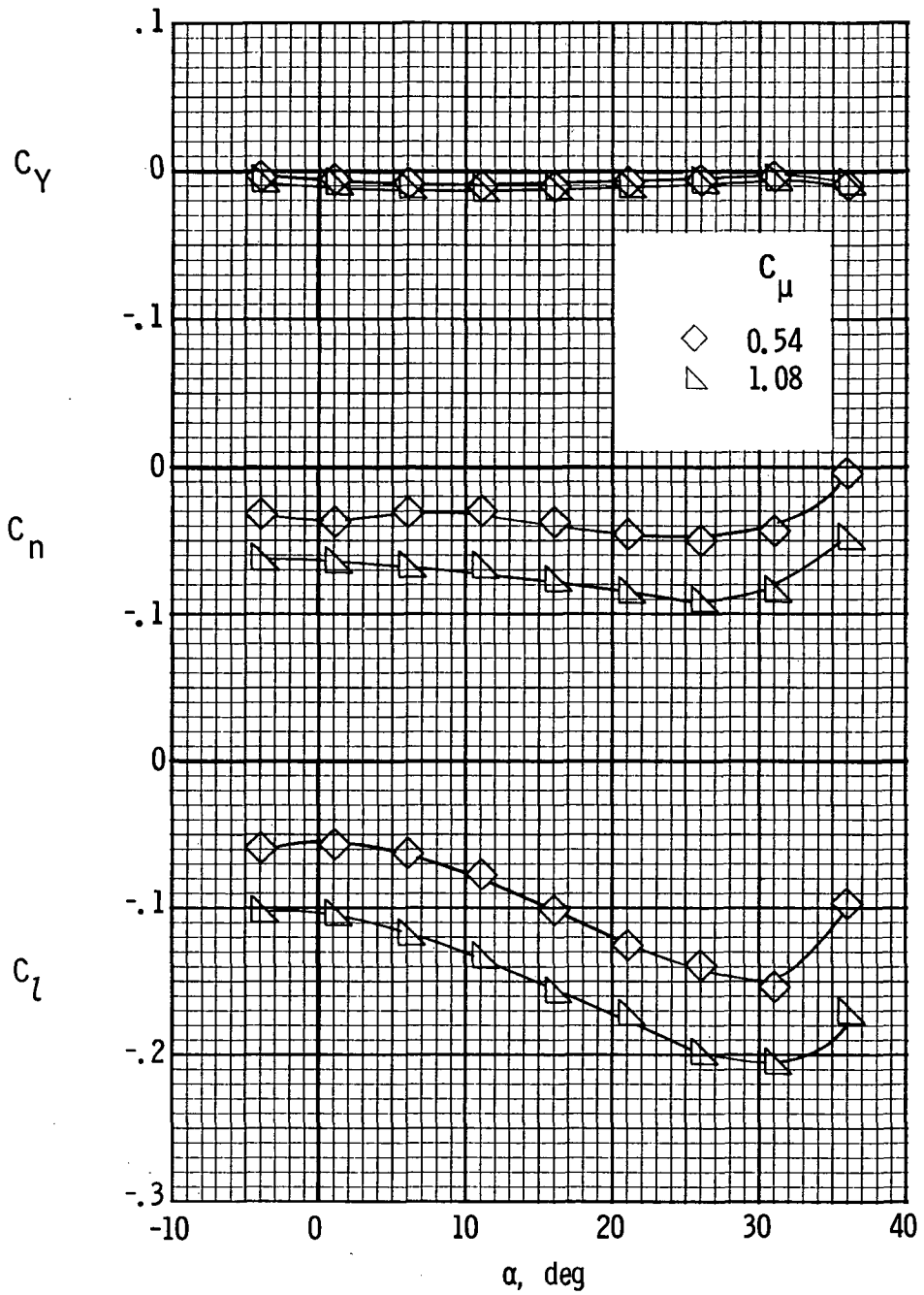
(a) Lateral characteristics.

Figure 25.- Lateral and longitudinal characteristics of two-engine model with left engine inoperative.  $\delta_f = 55^\circ$ ; tail off; trailing-edge flap slots closed behind engines.



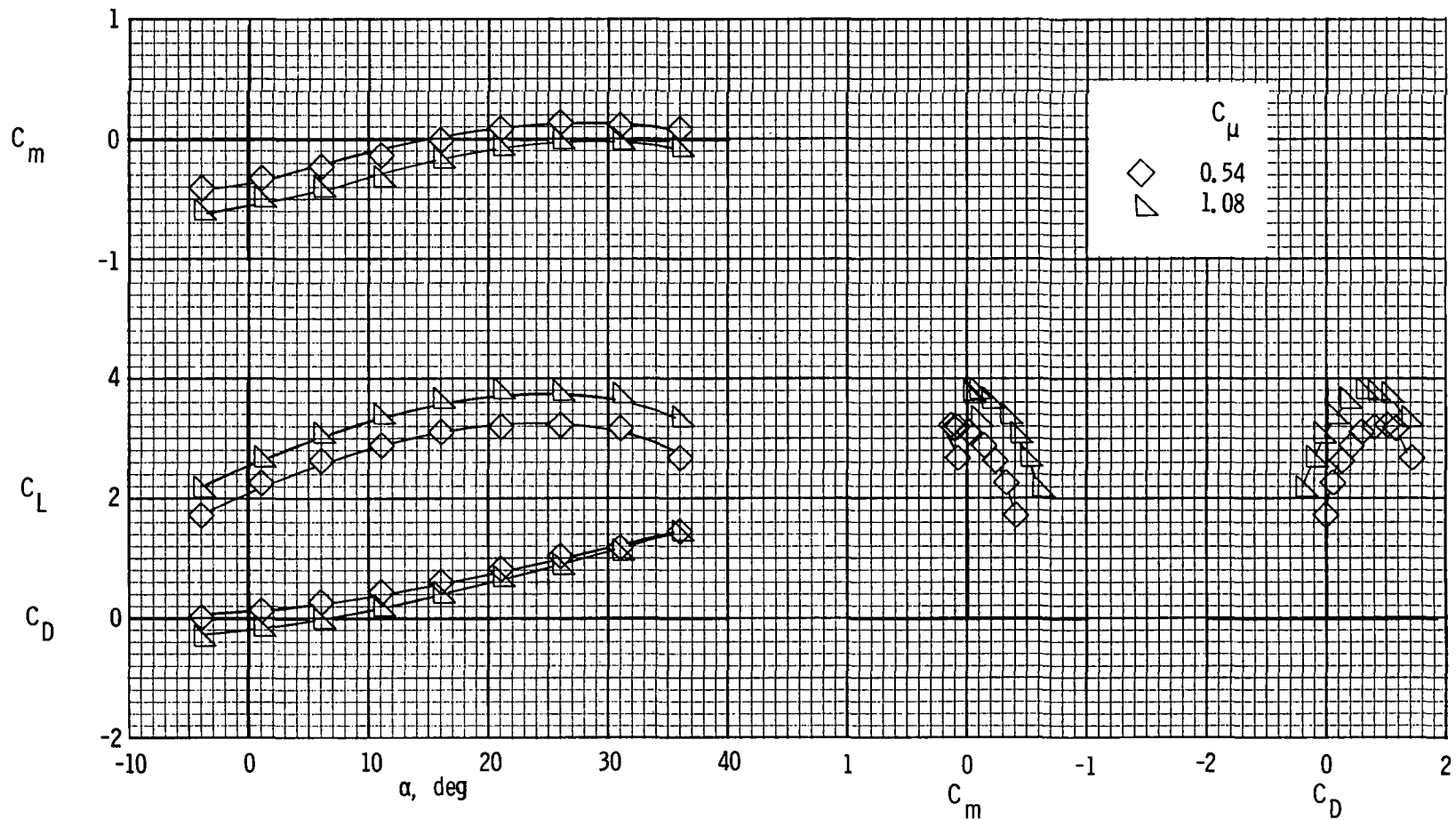
(b) Longitudinal characteristics.

Figure 25.- Concluded.



(a) Lateral characteristics.

Figure 26.- Lateral and longitudinal characteristics of two-engine model with left engine inoperative.  $\delta_f = 55^\circ$ ; tail off; trailing-edge flap slots open behind operative engine.



(b) Longitudinal characteristics.

Figure 26.- Concluded.

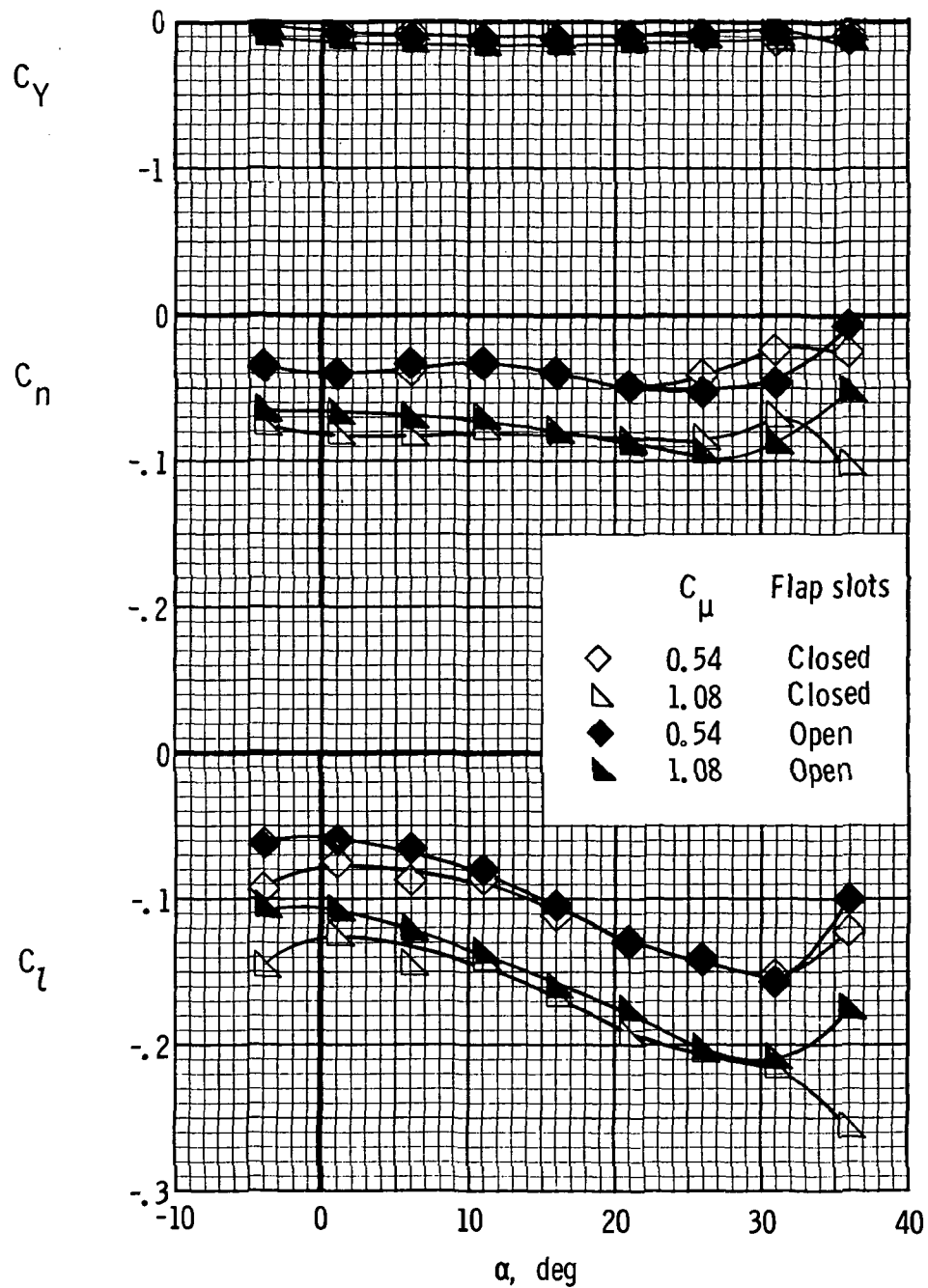


Figure 27.- Effect of closing trailing-edge flap slots behind inoperative engine for two-engine arrangement.  $\delta_f = 55^\circ$ ; tail off.

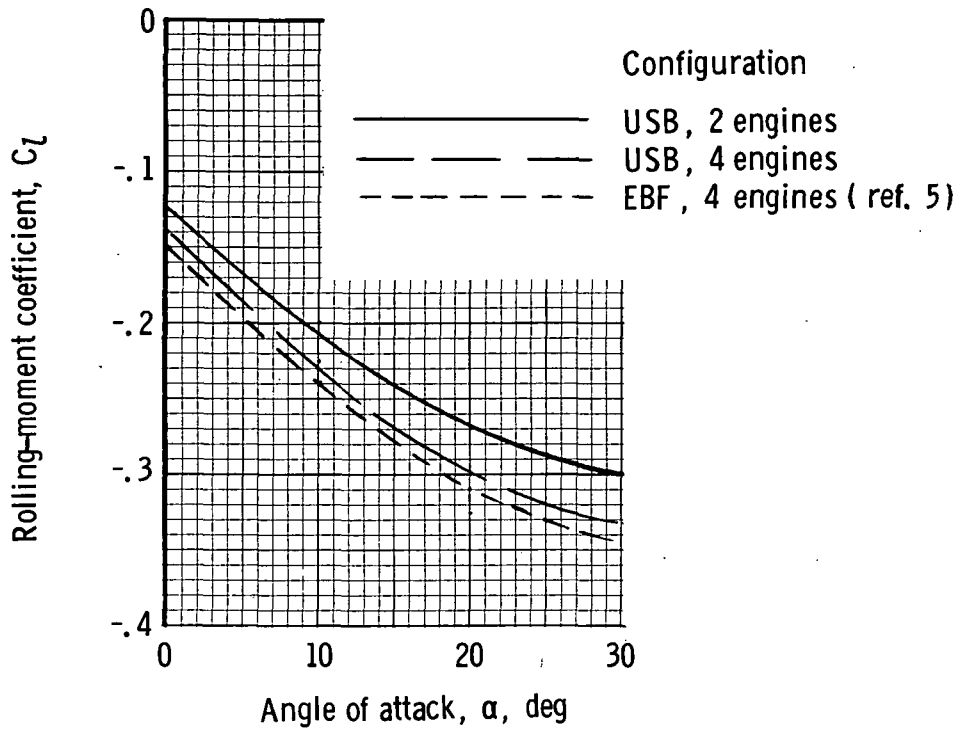
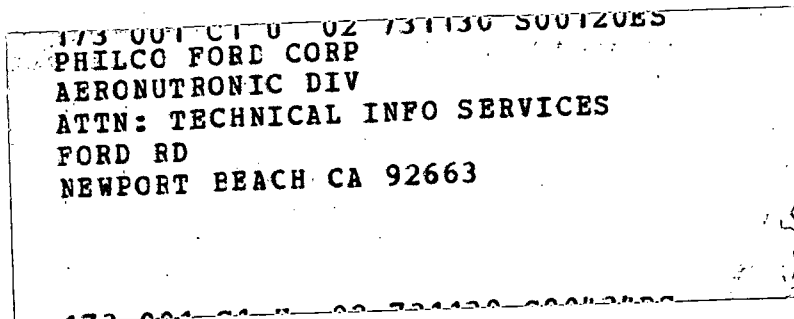


Figure 28.- Comparison of engine-out rolling moments for the upper surface blown jet-flap concept and the externally blown jet-flap concept.  $\delta_f = 55^\circ$ ; thrust-weight ratio, 0.45; left outboard engine inoperative.



POSTMASTER: If Undeliverable (Section 158  
Postal Manual) Do Not Return.

*"The aeronautical and space activities of the United States shall be conducted so as to contribute . . . to the expansion of human knowledge of phenomena in the atmosphere and space. The Administration shall provide for the widest practicable and appropriate dissemination of information concerning its activities and the results thereof."*

—NATIONAL AERONAUTICS AND SPACE ACT OF 1958

## NASA SCIENTIFIC AND TECHNICAL PUBLICATIONS

**TECHNICAL REPORTS:** Scientific and technical information considered important, complete, and a lasting contribution to existing knowledge.

**TECHNICAL NOTES:** Information less broad in scope but nevertheless of importance as a contribution to existing knowledge.

**TECHNICAL MEMORANDUMS:** Information receiving limited distribution because of preliminary data, security classification, or other reasons. Also includes conference proceedings with either limited or unlimited distribution.

**CONTRACTOR REPORTS:** Scientific and technical information generated under a NASA contract or grant and considered an important contribution to existing knowledge.

**TECHNICAL TRANSLATIONS:** Information published in a foreign language considered to merit NASA distribution in English.

**SPECIAL PUBLICATIONS:** Information derived from or of value to NASA activities. Publications include final reports of major projects, monographs, data compilations, handbooks, sourcebooks, and special bibliographies.

**TECHNOLOGY UTILIZATION PUBLICATIONS:** Information on technology used by NASA that may be of particular interest in commercial and other non-aerospace applications. Publications include Tech Briefs, Technology Utilization Reports and Technology Surveys.

Details on the availability of these publications may be obtained from:

**SCIENTIFIC AND TECHNICAL INFORMATION OFFICE**

**NATIONAL AERONAUTICS AND SPACE ADMINISTRATION**

Washington, D.C. 20546